

# CHAPTER 11 INSTRUMENTATION

---

<b>11.1</b>	<b>Introduction</b> .....	508
<b>11.2</b>	<b>Load Measuring Devices</b> .....	508
11.2.1	Flat Jacks and Pressure Cells .....	508
11.2.2	Load Cells .....	509
<b>11.3</b>	<b>Stress-Measuring Devices</b> .....	510
11.3.1	Absolute In-Situ Stress Measurement .....	512
11.3.2	Stress Change Measurement .....	523
<b>11.4</b>	<b>Deformation-Measuring Devices</b> .....	529
11.4.1	Convergence Meters .....	529
11.4.2	Differential Roof Sag Meters .....	532
<b>11.5</b>	<b>Strain-Measuring Devices</b> .....	536
<b>11.6</b>	<b>Bearing Capacity of the Roof and Floor</b> .....	537
<b>11.7</b>	<b>Borehole Observation Devices</b> .....	540
<b>11.8</b>	<b>Overburden Strata Movement Monitoring Devices</b> .....	541
11.8.1	Wireline Bullet Perforations .....	541
11.8.2	Time Domain Reflectometry (TDR) .....	541
11.8.3	Multi-position Borehole Extensometer (MPBX) .....	543
11.8.4	Full-Profile Borehole Inclinator (FPBI) .....	545
<b>11.9</b>	<b>Longwall Shield Monitoring Devices</b> .....	548
<b>11.10</b>	<b>Borehole Penetrometer</b> .....	550

---

## 11.1 INTRODUCTION

Since ground control deals with the stability of mine structures by analyzing the imposed stress (or load) configurations and the induced strain or deformation in each structural element, knowledge of the distribution of stress and strain is of the utmost importance. The exact magnitude of stress or strain can be obtained by analytical modeling or by measuring strain characteristics of each structural element, which as discussed in Chapter 12 (p. 553), involves uncertainties in extrapolating lab-measured data to field conditions unless in-situ measurements are performed. But in-situ testing, or field instrumentation, is time-consuming and, in most cases, costly. On the other hand, field instrumentation has the advantage of obtaining measurements of stresses or strains directly.

Basically two types of instrumentation are used to obtain ground control data: one for measuring loads or stresses and the other for measuring deformation or strain. In addition to the basic requirements of low cost, simplicity, reliability, and adequate precision, a device for ground control instrumentation has to be rugged and unaffected by dust, dirt, water, moisture, shock, or vibration because of the hostile environments in underground coal mines. A device also has to be drift free, especially for those instruments used for measuring changes in load (or stress) or deformation (or strain) over an extended period of time.

In the following first four sections, instrumentation devices are discussed under four categories: load, stress, deformation, and strain. Since a great variety of instrumentation devices are used by each individual investigator in each category, only those instruments that have been commonly used in coalfields will be discussed.

## 11.2 LOAD MEASURING DEVICES

### 11.2.1 Flat Jacks and Pressure Cells

Flat jacks are thin-walled, hydraulic-oil-filled metal containers (Fig. 11.2.1). They are widely used for underground load measuring because they are simple to fabricate and can be made in various forms to fulfill most installation requirements. They are commonly made of two identical pieces of malleable sheet metal brazed or welded along the edges. A flat jack can also be made out of circular tubing of the proper size and length by compressing it into a flat cell and brazing or welding it along the top and bottom edges. The air inside the cell is then driven out and filled with hydraulic fluid. A pressure gauge is generally attached to the cell for pressure readings. The total load on the cell corresponding to each pressure reading is calibrated with a testing machine. Copper, brass, and mild steel have been used for this purpose. Various sizes and shapes of flat jacks have been made and used (Obert and Duvall, 1967). They range from 2 x 8 in. (50.8 x 203.2 mm) to 48 x 60 in. (1.2 x 1.5 m), depending on the purpose. The maximum pressure a cell can withstand will depend on the type and thickness of the body metal and the brazing or welding technique. A maximum pressure of 8,500 psi (58.6 MPa) was reported (Panek and Stock, 1964). However field measurements of pillar stresses over 10,000 psi (69 MPa) have been obtained (Campoli et al, 1990).

Pressure cells can be used to measure the loads on posts, cribs, and roof bolts. To ensure uniform pressure distribution during installation, each pressure cell is generally sandwiched between two flat steel plates before inserting it between the roofline and the post, between crib blocks, or between the roofline and the bearing plate of a roof bolt. A U-shaped pressure cell is usually made for the roof bolts.



Fig. 11.2.1 Load cells

### 11.2.2 Load Cells

Load cells are probably the most widely used devices for measuring loads in every subject field of load instrumentation. They consist of a metal annular ring to which at least four electrical resistance strain gauges are mounted on the inner surface of the ring. Among the four gauges, two are mounted vertically in a diametrical location perpendicular to the vertical gauges (Fig. 11.2.2). The four gauges are then wired to form the four arms of a Wheatstone bridge. This type of wiring is temperature compensated, i.e., it eliminates the effect of temperature changes. The load-sensing direction is vertical and parallel to the axis of the annular ring. Load cells are also calibrated with a testing machine or proving ring.

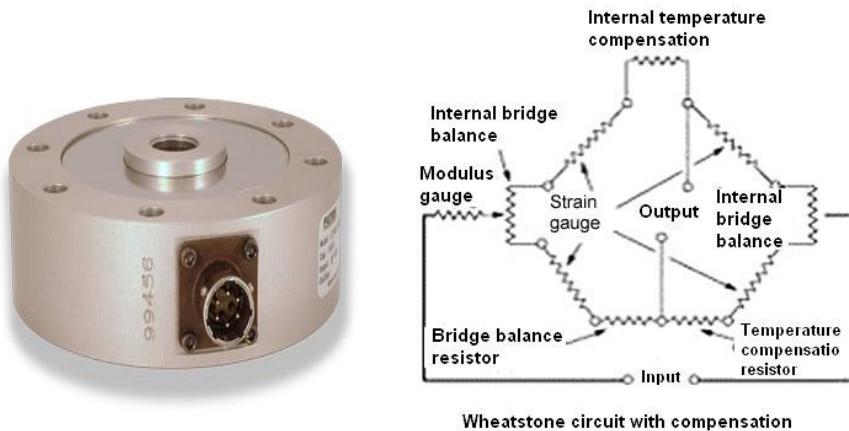


Fig.11.2.2 Load cell: left, overall view; and right, wheatstone bridge circuit

Figure 11.2.3 is a vibrating wire load cell (Song et al., 1982). When the load “P” is applied on the pressure membrane, it deforms and pulls the supporting rods apart. The length of the wire mounted between the two rods increases, and consequently its resonant frequency changes. When the magnetic coil in the exciter is excited, a wave is generated, which, in turn, causes the wire to vibrate in its resonant frequency. The signal is picked up by the receiver and displayed on a readout meter. Generally, the frequency is inversely proportional to the wire

length. Thus, once the calibration to correlate the wire frequency and applied load is made, the readout meter can be made to display the applied load directly. The maximum capacity of the vibrating wire load meter is 55 tons. It can be used to measure prop loads or canopy loadings of the shield supports. The vibrating wire load cells can be set up for automatic remote monitoring.

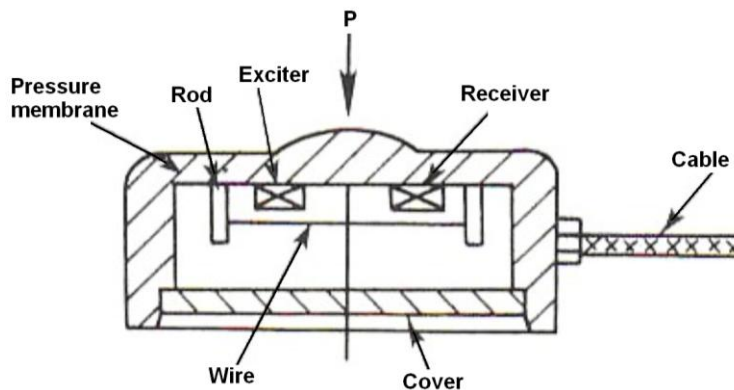


Fig. 11.2.3 Vibrating wire load cell (Song et al., 1982)

### 11.3 STRESS-MEASURING DEVICES

Stress-measuring devices are further classified into those that measure absolute in-situ stresses and those that measure changes in in-situ stresses, although any stress change can be obtained by the difference between two separate, absolute in-situ stress measurements.

The magnitude of in-situ stresses and strains experienced by each point in an underground rock mass subjected to external loading can be determined by measuring the amount of stress or strain released when the rock mass at the measuring point is separated from the surrounding rock mass. Methods of relieving rock stress or strain depend on location. If the stresses to be measured are on or near the surface of the opening, either slotting or overcoring is used, whereas overcoring or borehole trepanning or hydraulic fracturing is used for measurements far inside the surface of the openings.

In overcoring, the common procedure is first to drill a pilot hole into the wall of the opening until it reaches a depth equaling at least one opening width. A strain or displacement measuring device is then inserted into the hole or glued onto the wall or bottom end of the hole. Finally, the pilot hole or the bottom end is overcored, the strain or displacement changes before and after overcoring are recorded and converted to the state of stresses at the measuring point, through mainly the theory of elasticity. In-situ stress measurement devices utilizing overcoring concept include (Fig. 11.3.1): borehole deformation gauge (Hiramatsu and Oka, 1962), doorstopper (Leeman, 1964 and 1969), hollow inclusion (HI) cells (Dean, 1978), three-component borehole deformation gauge (Bickel, 1985; Hooker and Bickel, 1974), and triaxial cell (Kim and Frankling, 1987). In this section only the HI cell and three-component borehole deformation gauge will be described in detail due to their common usage for coal mine ground control designs.

It must be emphasized that the underlying principle of the overcoring method for stress measurements is to assume that underground rock strata are perfect elastic materials, i.e., upon unloading, the material follows the original loading curve and returns to the original zero

loading condition instantaneously. In underground coal mines, this assumption in most cases is not true. In fact, most coal measure strata exhibit time-dependent behavior of varying degrees. The overcoring method of stress measurement also assumes that all materials are homogenous and isotropic. On the contrary, all coal measure strata are at the minimum a transverse-isotropic material, i.e., the rock mechanics properties perpendicular to the bedding planes (or laminations) differ from those along the bedding planes (or laminations), and the properties are the same in all directions on the bedding plane (lamination). It is not known and few studies have been done regarding the difference between assuming the materials are perfectly elastic, and isotropic and assuming the materials are inelastic and transverse isotropic.

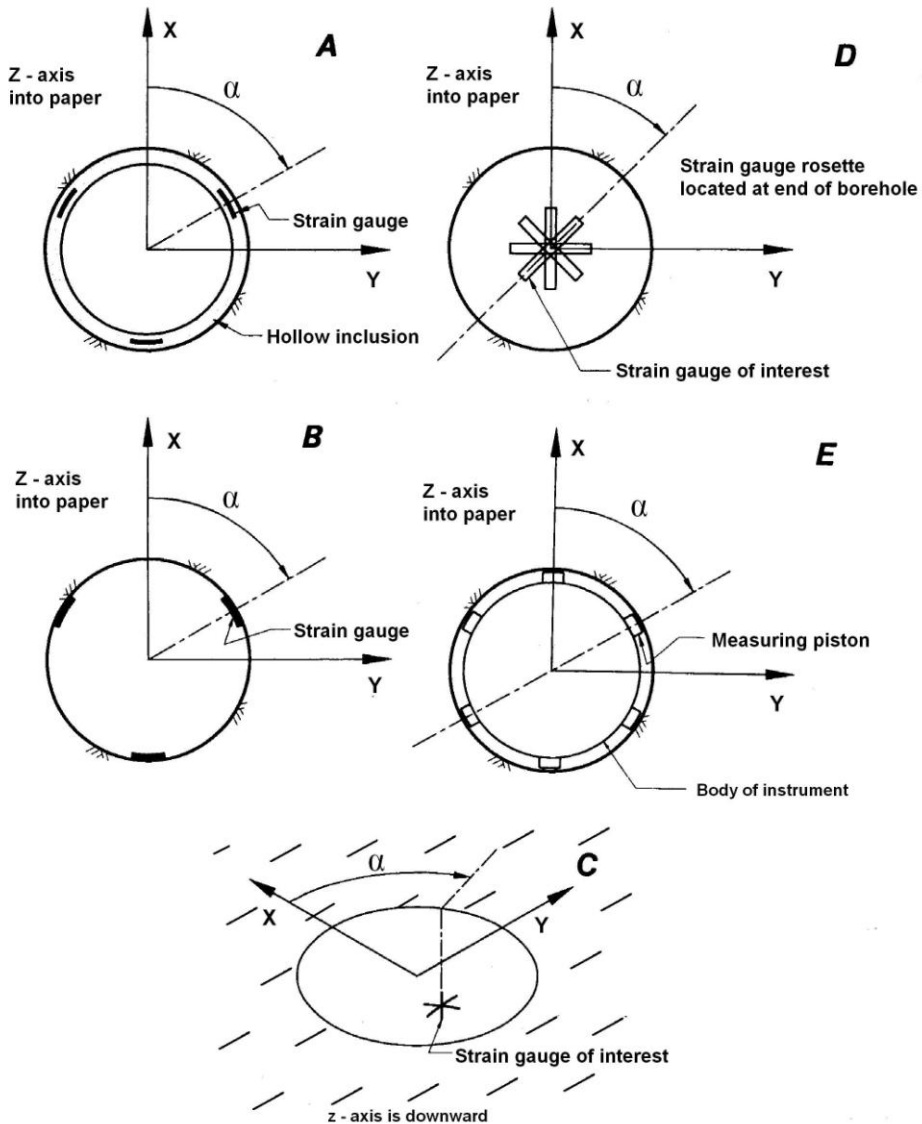


Fig. 11.3.1 Schematics showing five types of overcoring methods for in-situ stress measurement (Larson, 1992)

### 11.3.1 Absolute In-Situ Stress Measurement

#### 1. Flat Jacks

Flat jacks are used in determining in-situ stresses in opening sidewalls. Figure 11.3.2 shows the procedures used in this method (Leeman, 1964). First, two pins, A and B, are installed in the area for which stress is to be measured. The distance,  $X$ , between A and B is measured to the nearest 0.0001 in. (0.00254 mm). A horizontal slot is cut into the rock either above or below the pins at a vertical distance  $L/3$ , where  $L$  is the width of the slot. The slot must be sufficiently deep to eliminate edge effect. Once the slot is completed, the distance,  $X$ , increases an amount  $\Delta X$  due to the release of the vertical stress perpendicular to the slot. A flat jack is cemented into the slot, and pressure is applied until the distance AB is again reduced to  $X$ . The pressure at this time is assumed to be the original vertical pressure. The slot must be sufficiently wide and deep to eliminate the edge effect.

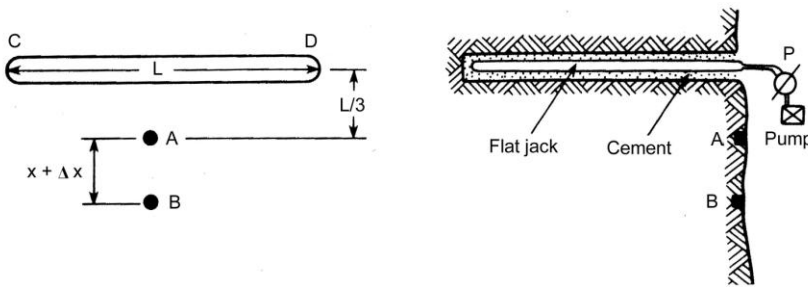


Fig. 11.3.2 In-situ stress measurement by the flat jack method (Leeman, 1964)

This method can only be used to determine stress perpendicular to the slot. Alternatively, the slot is cut in the center between points A and B, but the distance between the pins must be such that both pins are located at a distance  $L/3$  from the slot.

Since it is well-known that stresses in the strata in the immediate vicinity of an opening are highly non-uniform, this method measures the average stress over the area of the flat jack, ignoring the high stress gradient in the area.

#### 2. Borehole Deformation Gauge

When a circular hole is drilled parallel to one of the primary principal stresses (Fig. 11.3.3) in an ideal elastic body, the diametrical deformation or change in diameter  $U$  is (Merrill, 1967)

$$U = \frac{D}{E} [(\sigma_1 + \sigma_2) - \nu\sigma_3 + 2(\sigma_1 - \sigma_2)\cos 2\theta_p] \quad (11.3.1)$$

where  $D$  is the diameter of the borehole,  $E$  is the Young's Modulus of the material, and  $\nu$  is its Poisson's ratio,  $\sigma_1$  and  $\sigma_2$  are the secondary major and minor principal stresses in the plane perpendicular to the axis of the borehole, and  $\theta_p$  is the angle between  $\sigma_1$  and the diametrical direction along which change in diameter is of interest. Since there are 4 unknowns in Equation 11.3.1, 4 measurements, i.e., 3 diametrical deformations in three specified directions, and an axial deformation, are required. Various borehole deformation gauges have been developed for this purpose. Some measure a single diametrical deformation, some measure two orthogonal diametrical deformations in either one or two planes, and some measure three diametrical deformations in three specified directions in a single plane (Leeman, 1964).

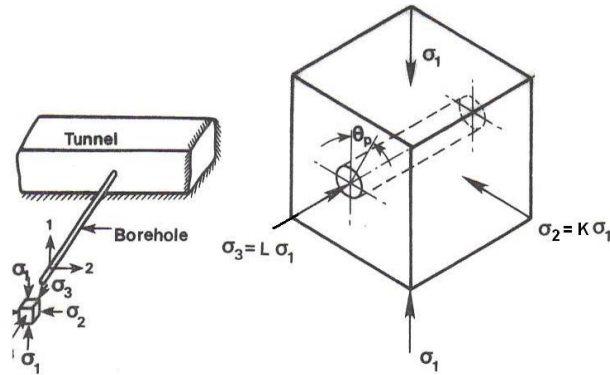
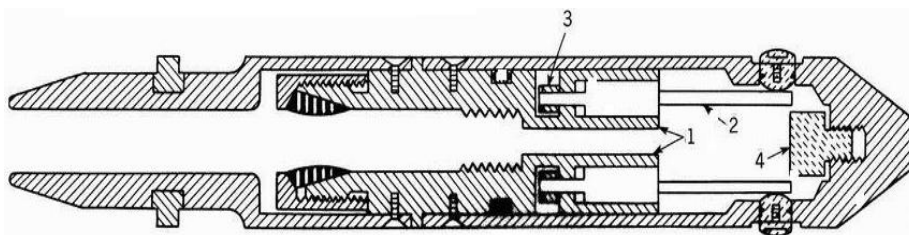


Fig. 11.3.3 Symbol used in the borehole method of in-situ stress determination (Leeman, 1964)

If it is assumed that the primary minor principal stress  $\sigma_3$  is parallel to the axis of the borehole and negligibly small, only three measurements are needed for solving Equation 11.3.1. The three-component borehole deformation gauge developed by the U.S. Bureau of Mines (now NIOSH) is designed for this purpose and appears to be the most versatile (Fig. 11.3.4). It operates on the principle that if three diameter deformations at  $60^\circ$  intervals are measured, the magnitude and orientation of the (secondary) major ( $\sigma_1$ ) and minor ( $\sigma_2$ ) principal stresses in a plane perpendicular to the axis of the borehole can be determined by the following equations (Merrill, 1967). The principal stresses so measured are called **secondary principal stresses**, because they are those applied on a specified plane.



Longitudinal section

- 1 Gage body with tapered mounts
- 2 Tapered mounted transducer
- 3 Locking nut
- 4 Safety plug

Fig. 11.3.4 The three-component borehole deformation gauge developed by U.S. Bureau of Mines (now NIOSH)

$$\sigma_1 = \frac{E}{6D} \left\{ U_1 + U_2 + U_3 + \frac{\sqrt{2}}{2} \left[ (U_1 - U_2)^2 + (U_2 - U_3)^2 + (U_3 - U_1)^2 \right]^{\frac{1}{2}} \right\} \quad (11.3.2)$$

$$\sigma_1 = \frac{E}{6D} \left\{ U_1 + U_2 + U_3 - \frac{\sqrt{2}}{2} \left[ (U_1 - U_2)^2 + (U_2 - U_3)^2 + (U_3 - U_1)^2 \right]^{\frac{1}{2}} \right\} \quad (11.3.3)$$

$$\theta_p = \frac{1}{2} \tan^{-1} \left[ \frac{-\sqrt{3}(U_2 - U_3)}{2U_1 - U_2 - U_3} \right] \quad (11.3.4)$$

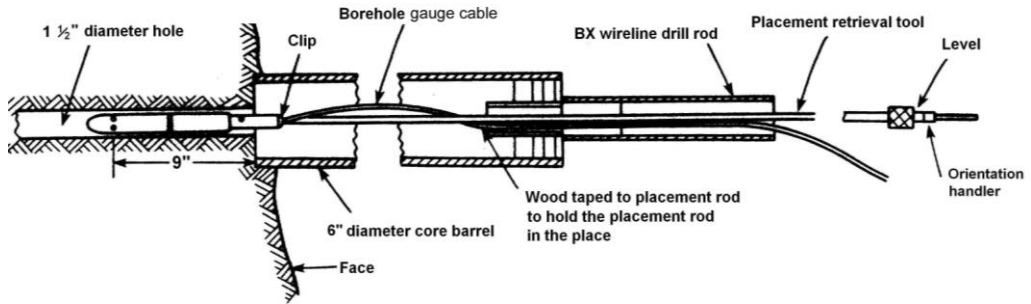
where  $U_1$ ,  $U_2$ , and  $U_3$  are the diametrical deformation for direction 1, 2, and 3, respectively,  $D$  is the diameter of the borehole, and  $\theta_p$  is the acute angle between the direction of  $U_1$  and  $\sigma_1$ .

Figure 11.3.4 (lower) is a cross-sectional view of the three-component deformation gauge (Bickel, 1985). The deformation sensing devices are six pieces of heat-treated beryllium-copper strips mounted on six cantilevers. The six strips are located in three diametrical directions at  $60^\circ$  intervals. Two strain gauges, one on the top and the other on the bottom, are mounted in each strip near the clamped ends. The four strain gauges on each two diametrically located strips are wired to form a four-arm wheatstone bridge circuit, whose strain outputs are calibrated to indicate the amounts of deflection for the two strips. The deflections of the cantilever strips are caused by the movement of pistons that, due to their spring action, are always in intimate contact with the wall of the borehole. During borehole overcoring, those strain-gauged cantilevered beams will rebound registering the expansion of the borehole diameter.

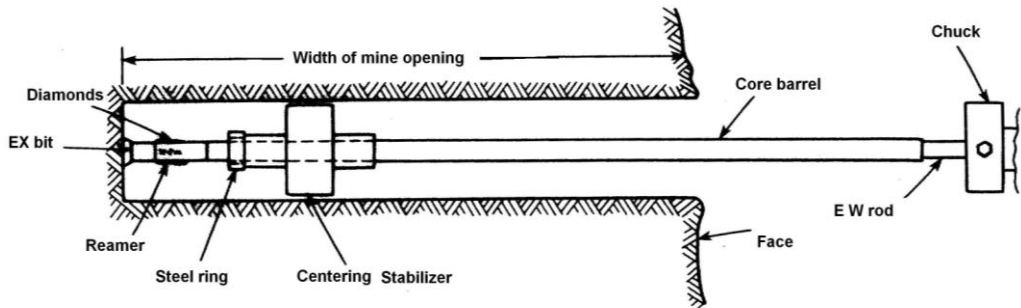
The operational procedures of in-situ stress measurement using the three-component borehole gauges are shown in Fig. 11.3.5 (Bickel, 1985). First a 1.5 in. diameter (EX) hole is drilled to a depth approximately 1 ft (0.3 m) past the point where the measurement is intended. The borehole gauge is then inserted until the location of the pistons coincides with the point of measurement. At this time each strain gauge is fully balanced and adjusted to a zero reading. A 6 in. (152.4 mm) diameter core is next overcored concentrically with the EX hole to release the pressure applied to the core between the two holes. The release is believed to be complete when the bottom of the 6 in. (152.4 mm) diameter hole is 9 in. (228.6 mm) past the location of the gauge pistons. The strain gauge readings at this moment subtracted from the corresponding zero readings correspond to the total increases in diameter of the EX hole due to the complete stress-release of the core. They are used in Equations 11.3.2 to 11.3.4 to calculate  $\sigma_1$ ,  $\sigma_2$  and  $\theta_p$ . Since each overcoring measures only the principal stresses located in the planes perpendicular to the axis of the borehole, the determination of the complete state of stress at a point requires three overcoring at three different orientations. Several borehole configurations for determining the complete state of stress at a point in an underground opening are shown in Fig. 11.3.6. To determine the undisturbed in-situ stresses, the borehole must be drilled and measurements made at a distance at least one and one-half diameter (or width) inside the roof or rib or floor to get rid of the disturbance due to the existence of the opening. An overcored hole of at least 10 in. (254 mm) must be used in overcoring coal. Otherwise, the core tends to break up because of the abundance of mutual fractures in coal.

The core recovered from the overcoring is then subjected to biaxial testing to determine the rock properties of the rock strata where stress measurements are performed. These rock properties are required for solving Equations 11.3.2-11.3.4. A general purpose software stress OUT is available for solving the complicated equations associated with each overcoring method (Larson, 1992).





A - Positioning the 3-D borehole gauge with the placement rod through the 6" diameter core barrel and stem



B - Starting the 1 1/2" diameter hole in the bottom of the 6" diameter hole

Fig. 11.3.5 Operational procedures of in-situ stress determination using three-component borehole deformation gauge developed by the U.S. Bureau of Mines (now NIOSH)

### 3. Hollow Inclusion (HI) Cells

The Hollow Inclusion (HI) cell is a soft inclusion type of stressmeter. The measuring device consists of three strain gauge rosettes embedded in a thin wall epoxy cylinder, 1.5 in. (38 mm) in diameter. The three rosettes, consisting of a total of 9 strain gauges, are mounted at  $0^\circ$ ,  $90^\circ$ , and  $135^\circ$  around the circumference of the cylinder (Fig. 11.3.7). The 9-gauge cell is for determining stress fields in an isotropic rock mass. For an anisotropic rock mass, 12 gauges are required (Amadei, 1985 and 1986; van Heerden, 1983). A strain gauge rosette consists of three strain gauges oriented at three different locations, normally one each at vertical, horizontal, and  $45^\circ$  directions, for determining the principal strains in two dimensions.

The strains in the cell at position  $(\rho, \theta)$  are (Fig. 11.3.8) (Duncan-Fama and Pender, 1980)

$$E_z e_\theta = [\sigma_x^o + \sigma_y^o] K_1(\rho) - \nu_2 \sigma_z^o K_4(\rho) - 2[1 - \nu_2^2] \left\{ \sigma_x^o - \sigma_y^o \right\} \cos 2\theta + 2\tau_{yz}^o \sin 2\theta \} K_2(\rho) \quad (11.3.5)$$

$$E_2 e_z = \sigma_z^o - \nu_2 (\sigma_x^o + \sigma_y^o) \quad (11.3.6)$$

$$E_2 \gamma_\alpha = 4(1 + \nu_2) (-\tau_{xz}^o \sin 2\theta + \tau_{yz}^o \cos \theta) K_3(\rho) \quad (11.3.7)$$

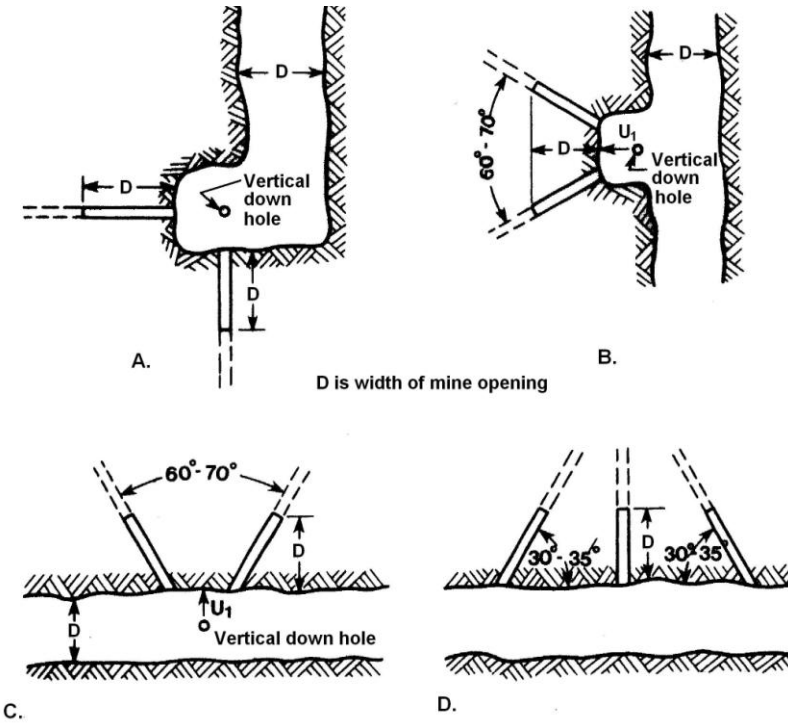


Fig. 11.3.6 Various drill hole configurations for determining the complete state of in-situ stress: D is opening width

where

$$K_1(\rho) = d_1(1 - \nu_1\nu_2) \left( 1 - 2\nu_1 + \frac{R_1^2}{\rho^2} \right) + \nu_1\nu_2 \tag{11.3.8}$$

$$K_2(\rho) = (1 - \nu_1)d_2\rho^2 + d_3 + \frac{\nu_1d_4}{\rho^2} + \frac{d_5}{\rho^4} \tag{11.3.9}$$

$$K_3(\rho) = d_6 \left( 1 + \frac{R_1^2}{\rho^2} \right) \tag{11.3.10}$$

$$K_4(\rho) = -\frac{(\nu_1 - \nu_2)d_1}{\nu_2} \left( 1 - 2\nu_1 + \frac{R_1^2}{\rho^2} \right) + \frac{\nu_1}{\nu_2} \tag{11.3.11}$$

where  $\rho$  is the radial coordinate at the position of strain gauges, the  $K$  factors were introduced by Worotnicki and Walton (1976),  $d_1, d_2, d_3, d_4, d_5,$  and  $d_6$  are constants for stresses in the epoxy,  $e_r, e_\theta, e_z, \gamma_{r\theta}, \gamma_{\theta z},$  and  $\gamma_{zr}$  are strains,  $E_1$  and  $E_2$  are Young's Modulus for the epoxy and rock, respectively,  $\nu_1$  and  $\nu_2$  are poisons ratio of epoxy and rock, and  $R_1$  and  $R_2$  are the inner radius for the cylinder and pilot hole, respectively. Note that in  $\sigma_x^o, \sigma_y^o, \sigma_z^o,$  and  $\tau_{xy}^o,$  the superscripts denote strain gauge location.

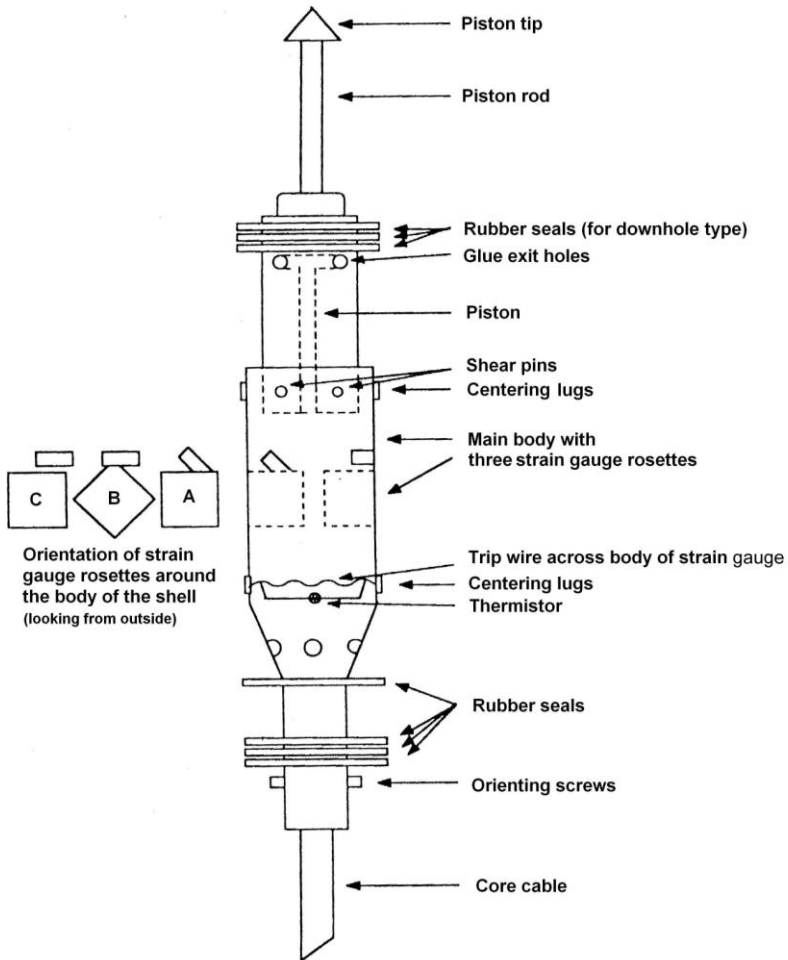


Fig. 11.3.7 Construction details of hollow inclusion (HI) cell (Mindata Australia, 1987)

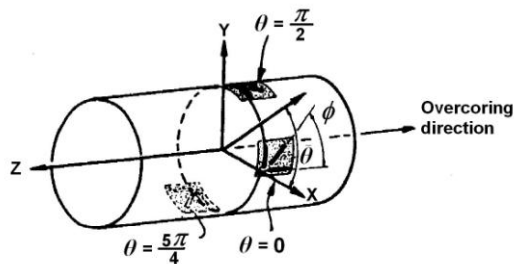


Fig. 11.3.8 Symbols for hollow inclusion cell (Duncan-Fama and Pender, 1980)

At  $\theta=0^\circ$  and  $\theta=(5\pi/4)^\circ$ , the three gauges are mounted in directions  $\phi=0^\circ, (\pi/2)^\circ$ , and  $(\pi/4)^\circ$ . At  $\theta=(\pi/2)^\circ$ , the three gauges are mounted in direction  $\phi=0^\circ, (\pi/2)^\circ$ , and  $(1\pi/4)^\circ$ .

The gauges at  $\phi=0$  measure  $e_z$ ; the gauges at  $\phi=(\pi/2)^\circ$  measure  $e_\theta$ , and the gauges at  $\phi=(\pm\pi/4)^\circ$  measure  $e_{45} = \frac{1}{2}(e_\theta + e_z \pm \gamma_{\theta z})$ . The three gauge measurements at  $\phi=0^\circ$  are averaged to give a most probable value for  $e_z$ . This value plus the three  $e_\theta$  values are used to determine  $\sigma_x^o, \sigma_y^o, \sigma_z^o$ , and  $\tau_{xy}^o$  from the following equations:

$$E_2 e_z = \sigma_z^o - \nu_2 (\sigma_x^o + \sigma_y^o) \quad (11.3.12)$$

$$E_2 e_\theta(0) = (\sigma_x^o + \sigma_y^o) \cdot \overline{K_1} - (\sigma_x^o - \sigma_y^o) \cdot \overline{K_2} - \sigma_z^o \overline{K_4} \quad (11.3.13)$$

$$E_2 e_\theta\left(\frac{\pi}{2}\right) = (\sigma_x^o + \sigma_y^o) \cdot \overline{K_1} + (\sigma_x^o - \sigma_y^o) \overline{K_2} - \sigma_z^o \overline{K_4} \quad (11.3.14)$$

$$E_2 e_\theta\left(\frac{5\pi}{4}\right) = (\sigma_x^o + \sigma_y^o) \cdot \overline{K_1} - 2\tau_{xy}^o \cdot \overline{K_2} - \sigma_z^o \overline{K_4} \quad (11.3.15)$$

where

$$\overline{K_1} = K_1(\rho) \quad (11.3.16)$$

$$\overline{K_2} = 2(1 - \nu_2^2) K_2(\rho) \quad (11.3.17)$$

and

$$\overline{K_4} = \nu_2 K_4(\rho) \quad (11.3.18)$$

From Equations 11.3.12 to 11.3.18, the six components of the state of stress are,

$$\sigma_z^o = \frac{E_2}{(\overline{K_1} - \nu_2 \overline{K_4})} \left\{ \overline{K_1} e_z + \frac{\nu_2}{2} \left[ e_\theta(0) + e_\theta\left(\frac{\pi}{2}\right) \right] \right\} \quad (11.3.19)$$

$$\sigma_y^o = \frac{\sigma_z^o \overline{K_4}}{2\overline{K_1}} + \frac{E_2}{4\overline{K_1} \overline{K_2}} \left\{ (\overline{K_2} + \overline{K_1}) e_\theta(0) + (\overline{K_2} - \overline{K_1}) e_\theta\left(\frac{\pi}{2}\right) \right\} \quad (11.3.20)$$

$$\sigma_x^o = \frac{\sigma_z^o \overline{K_4}}{2\overline{K_1}} + \frac{E_2}{4\overline{K_1} \overline{K_2}} \left\{ (\overline{K_2} - \overline{K_1}) e_\theta(0) + (\overline{K_2} + \overline{K_1}) e_\theta\left(\frac{\pi}{2}\right) \right\} \quad (11.3.21)$$

$$\tau_{xy}^o = -\frac{1}{2\overline{K_2}} \left[ E_2 e_\theta\left(\frac{5\pi}{4}\right) + \sigma_z^o \overline{K_4} - (\sigma_x^o + \sigma_y^o) \overline{K_1} \right] \quad (11.3.22)$$

$$\tau_{xz}^o = \frac{E_2}{16(1 + \nu_2) \cdot \overline{K_3}} \left[ -3\gamma_{\theta z}\left(\frac{\pi}{2}\right) + \gamma_{\theta z}(0) + \sqrt{2}\gamma_{\theta z}\left(\frac{5\pi}{4}\right) \right] \quad (11.3.23)$$

$$\tau_{xz}^o = \frac{E_2}{16(1+\nu_2) \cdot K_3} \left[ 3\gamma_{\theta z}(0) - \gamma_{\theta z}\left(\frac{\pi}{2}\right) - \sqrt{2}\gamma_{\theta z}\left(\frac{5\pi}{4}\right) \right] \quad (11.3.24)$$

Therefore, an HI cell measures the complete state of stress at a point with one borehole as compared to three different holes in different directions with the three-component deformation gauge.

Figure 11.3.9 shows the procedure for stress measurement using the hollow inclusion (HI) cell.

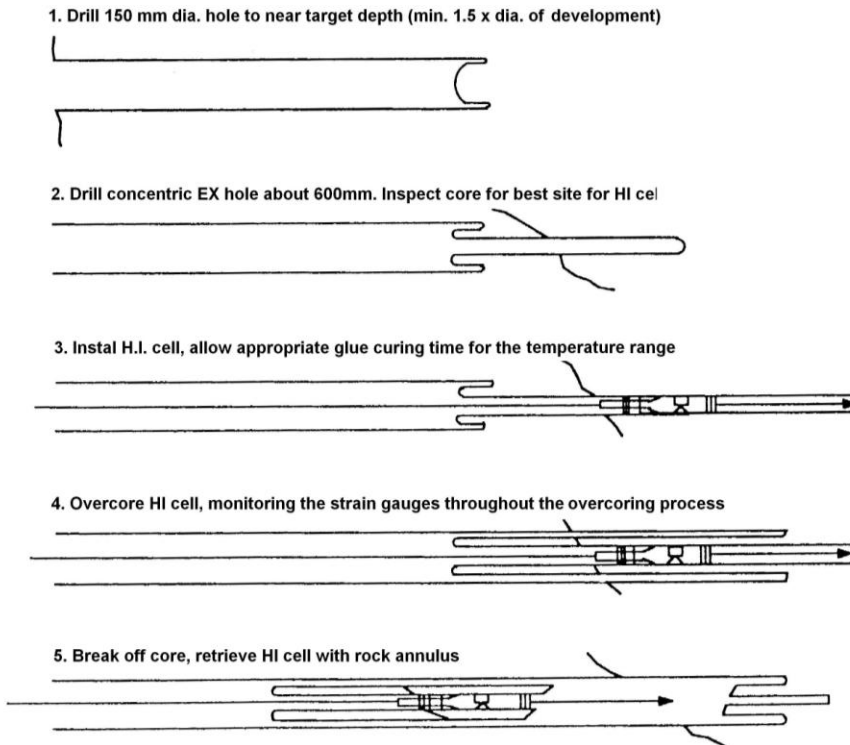


Fig. 11.3.9 Procedure of stress measurement using HI Cell (Mindata Australia, 1987)

#### 4. Hydraulic Fracturing

Hydraulic fracturing was developed for and has been used extensively by the petroleum industry for enhanced oil recovery (Howard and Fast, 1970). In this procedure, a section of a well is sealed off (Fig. 11.3.10) with a packer at both ends. Water is then pumped into this sealed section. The water pressure is increased continuously until a horizontal or vertical fracture is initiated in the surrounding rock. The rock fractures by tension and is perpendicular to the minimum principal stress, so the stress measured at the time of the rock fracture can be used to estimate the minor principal stress.

The stress fields at the time of rock fracturing are (Kehle, 1964; Obert and Duvall, 1967), at the ends of the pressurized section

$$\sigma_{\theta(total)} = 3\sigma_{h1} - \sigma_{h2} \quad (11.3.25)$$

$$\sigma_{z(total)} = R + 0.94 p \tag{11.3.26}$$

At the central part of the pressurized section

$$\sigma_{\theta(total)} = 3\sigma_{h1} - \sigma_{h2} + p \tag{11.3.27}$$

$$\sigma_{z(total)} = R \tag{11.3.28}$$

where  $R = \gamma h$  is principal vertical load,  $\gamma$  is rock density,  $h$  is depth,  $p$  is the hydrostatic water pressure,  $\sigma_z$  and  $\sigma_\theta$  are axial and tangential stress around the well, respectively, and  $\sigma_{h1}$   $\sigma_{h2}$  are the maximum and minor principal horizontal stresses, respectively.

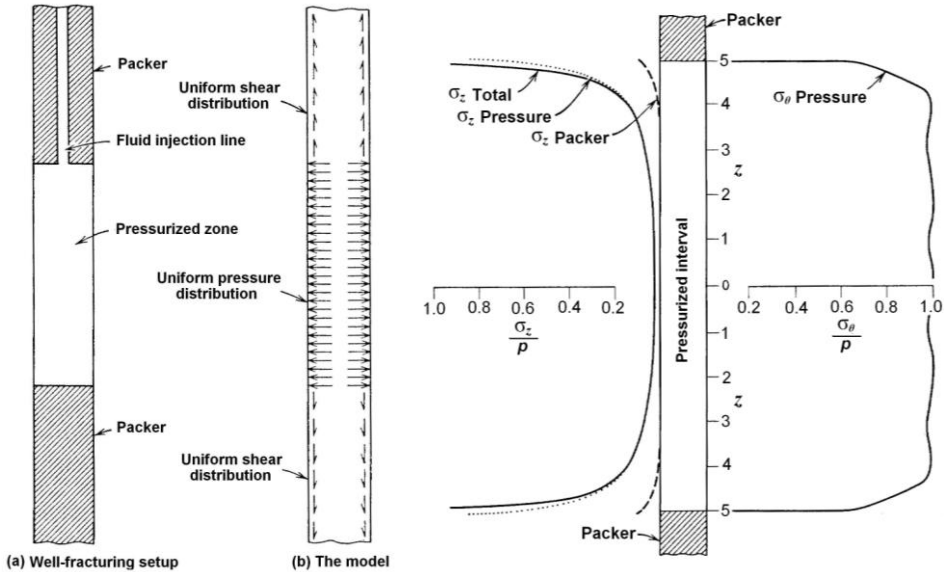


Fig. 11.3.10 Hydraulic fracturing: left, terminologies for the sealed section, and right, stress distributions in the sealed section (Kehle, 1964)

The well will fail when  $p$  reaches a critical value  $p_c$  equal or greater than the tensile strength of the rock,  $T_o$ . Since rock is much weaker in tension, tensile fracture will occur perpendicular to maximum tensile stress. Two types of fractures are possible:

- (1) If  $\sigma_{z(total)} = R + 0.94 p_c < T_o$ , fracture will occur in the central part of the sealed section when

$$\sigma_{\theta(total)} = 3\sigma_{h1} - \sigma_{h2} + p_c \geq T_o \tag{11.3.29}$$

the fracture will propagate perpendicular to  $\sigma_{\theta(total)}$ , i.e., in the vertical plane.

- (2) If  $\sigma_{\theta(total)} = 3\sigma_{h1} - \sigma_{h2} + p_c < T_o$ , fracture will initiate at the end when

$$\sigma_{z(total)} = R + 0.94 p_c \geq T_o \tag{11.3.30}$$

the fracture will propagate in a horizontal plane.

At shallow depths, e.g., 330-660 ft (100-200 m) deep, the vertical stress from rock weight constitutes the minimum principal stress in many cases. Under such conditions, fractures will initiate in the horizontal plane.

An impression packer inserted in the well after fracture initiation is used to determine the orientation of the fracture, which in turn, gives the orientation of the maximum secondary principal stress in the plane perpendicular to the hole axis.

Hydraulic fracturing has long been used for stress determination in coal mines (Dahl and Parsons, 1972). A standard testing method is available for in-situ stress measurement by surface borehole hydraulic fracturing (ASTM D 4645-97). The Minifrac system (Enever et al., 1990) (Fig. 11.3.11) is compact and popular for underground coal mine applications. The system includes a hydraulic fracture tool, an impression packer, installation rods, impression wrap material, a dual pump system, and a laboratory fracture strength test kit (Su and Hasenfus, 1995). The Minifrac tool is 1.42 in. (36 mm) in diameter with a test section 6.3 in. (160 mm) long. The impression packer is 1.42 in. (36 mm) in diameter and 19.7 in. (500 mm) long. Two pumps of 10,000 psi (69 MPa) are used to hydrofrac the test section with a hydraulic fluid comprised of a 19:1 ratio of clean water to water soluble oil. Fig. 11.3.12 shows an example of a test record using the Minifrac system (Su and Hasenfus, 1995).

The hydraulic fracturing method measures the two principal stresses (or secondary principal stresses) on a plane perpendicular to the borehole.

### 5. Rosette Displacement Gauge

Another simple, yet effective, method for measuring in-situ stresses on the surface of the opening is the rosette displacement gauge. It consists of a template for drilling a 60° rosette configuration, a 0.375 in. (9.5 mm) diameter rock drill bit for drilling holes for pin installation, six specially prepared stainless steel pins, and a Whitmore gauge (Fig. 11.3.13).

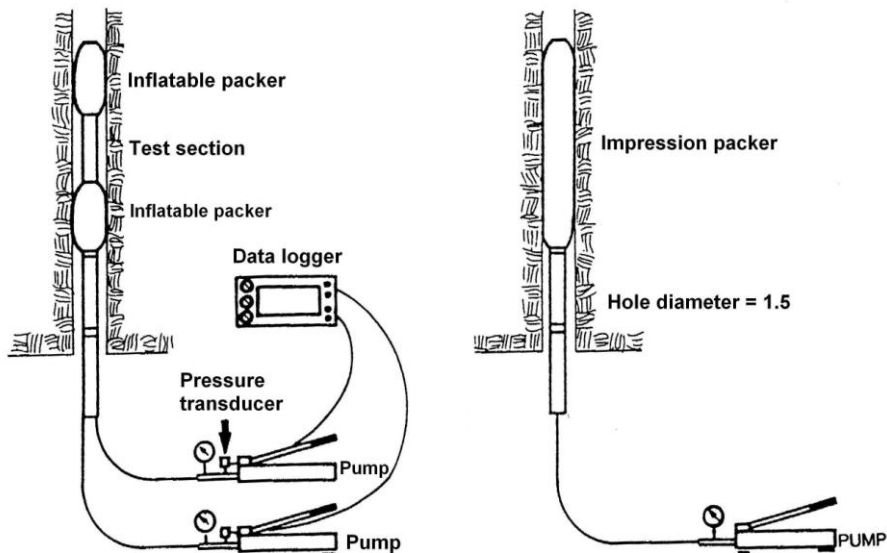


Fig. 11.3.11 The CSIRO Minifrac system (Enever et al., 1990)

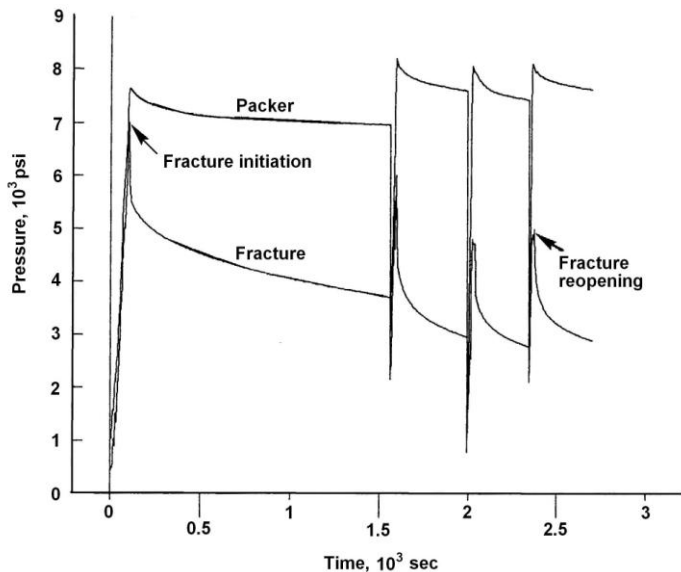


Fig. 11.3.12 An example of pressure/time record for the Minifrac test (Su and Hasenfus, 1995)



Fig. 11.3.13 Equipment for surface rosette displacement measurements

For best results the surface area where the stress measurement is to be made must be relatively smooth, intact, and free from visible fractures. The technique begins with marking the precise locations of the six pin holes using the template. The holes must be at least 4 in. (101.6 mm) deep. A stainless steel pin is inserted and glued into each hole (Fig. 11.3.14). The diametrical distances between each of the three pairs of the steel pins are measured with a Whitmore gauge. These are the original or reference diameters. A 0.5 in. (12.7 mm) diameter hole is then drilled at least 1 ft (0.3 m) deep at the center and reamed concentrically to become a 6 in. (152.4 mm) center hole. At this time the rock mass in the steel pins is totally stress relieved. The diametrical distance for each of the three pairs of the steel pins are measured again. The changes in diametrical distance for each pair of the steel pins are then determined. These changes in diametrical distance,  $U_1$ ,  $U_2$ , and  $U_3$ , are substituted into Equations 11.3.2-11.3.4 to obtain the secondary principal stresses,  $\sigma_1$  and  $\sigma_2$ , and their orientation,  $\theta$  on the surface where the measurement is performed.



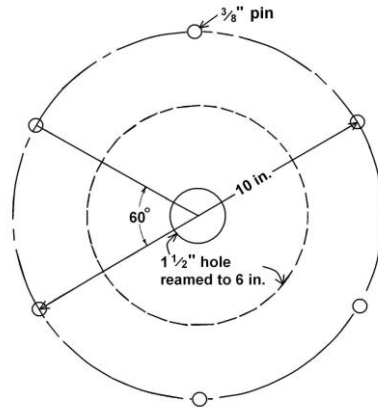


Fig. 11.3.14 Surface rosette configuration

In-situ stresses determined by this method are those acting on the surface of the opening. They are not the virgin in-situ stresses. However, the stresses so determined can be used for back-calculating the far-field in-situ virgin stresses through numerical computer modeling.

### 11.3.2 Stress Change Measurement

There are two types of devices that are commonly employed for measuring stress changes in underground coal mines: a vibrating wire stressmeter and an encapsulated pressure cell.

#### 1. Vibrating Wire Stress Meter

The vibrating wire stress meter consists of a high strength hollow cylinder into which a high strength thin wire is integrated diametrically by clamping (Fig. 11.3.15) (Hawkes, 1974). The wire is pre-tensioned. A coil, magnet, and yoke are used to vibrate the wire at its natural frequency. Since the natural frequency of a wire is proportional to the square root of the wire tension, which in turn is related to the length of the wire, a change in wire length due to the borehole diametrical change can be related to the changes in stresses applied on the borehole. During installation, the tensioned wire is oriented in a borehole 1.5 in. (38 mm) in diameter parallel to the direction for which change in stress is to be measured. The stress meter is preloaded by means of a sliding wedge and platen assembly. The wire tension is decreased and the frequency increased as the meter is set into the borehole using a special setting tool (Fig. 11.3.16B). The frequency further increases when the compressive stress on the borehole increases. The special readout meter (Fig. 11.3.16A), once connected to the gauge cable, will indicate the instantaneous frequency of the tensioned wire. Through laboratory calibration the changes in the frequency of the tensioned wire are related to the magnitude of stress changes in the host rock in the direction parallel to the tensioned wire. Changes in stress can also be determined by using the following equation suggested by the manufacturer:

$$\sigma_T = \frac{\left[ \frac{(422400)^2}{T_o} \right] \left( 1 - \frac{T_o}{T} \right)^2}{11.4 - 0.66 \times 10^{-6} E} \quad (11.3.31)$$

where  $\sigma_T$  is the change in uniaxial rock stress between the initial meter reading  $T_o$  and the current reading  $T$ , and  $E$  is the Young's Modulus of the rock.

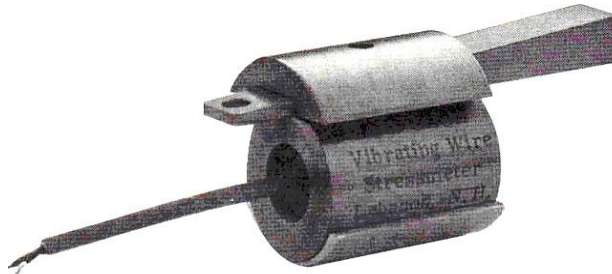
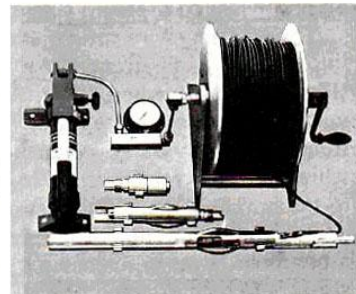


Fig. 11.3.15 Vibrating wire stressmeter (Hawkes, 1974)



A. MB-6 Vibrating wire Readout box



B. Hydraulic setting tool

Fig. 11.3.16 Readout meter (A) and hydraulic setting tool for vibrating wire stressmeter (Hawkes, 1974)

The vibrating wire stress meter is unidirectional, but the complete state of stress changes on a plane can be evaluated by installing three stress meters at different directions in a borehole. Vibrating wire stress meters are very sensitive and can be made to measure a maximum stress change of up to 8,000 psi (55.2 MPa). Gauge readings can be taken through cable miles long, and the readout meter needs only to be coupled to the gauge cable when readings are made. Alternatively, the output of a vibrating wire stress meter can be monitored remotely and automatically by a data logger. The data logger can scan at intervals ranging from continuous to 100 hours and print all recorded data on paper or stored on a compact disk (CD).

## 2. Borehole Pressure Cell (BPC) and Cylindrical Borehole Pressure Cell (CPC)

The borehole pressure cell (BPC) can also be used in the borehole to measure ground pressure changes. Figure 11.3.17 shows the flat pressure cell developed by the U.S. Bureau of Mines (1973) for boreholes 2.34 in. (59.4 mm) in diameter. The steel bladder is 2 in. (50.8 mm) wide by 8 in. (203.2 mm) long by 0.35 in. (8.9 mm) thick. During fabrication, two longitudinal holes of 0.5 in. (12.7 mm) outside diameter are normally cast in the concrete jacket, allowing the passage of hydraulic lines and the installation of several cells in a single hole. It is either grouted in place or encapsulated with a 2:1 sand-to-cement mortar to assume a cylindrical shape 2.34 in. (59.4 mm) in diameter by 8.75 in. (222.25 mm) long. During installation, the fluid pressure inside the cell is pumped to a certain level. As the pressure increases on the

borehole, the fluid pressure inside the cell is also proportionally changed. To convert an observed change of fluid pressure in the flat borehole pressure cell to the corresponding change of ground pressure, it is necessary to calibrate the response of the cell in that rock, in either the laboratory or in the field. The laboratory calibration method is done by setting the cell inside a 6 in. (152.4 mm) diameter core and observing the pressure response of the cell as the core is subjected to varying loads. The ratio of cell pressure change from the initial setting to the corresponding change in external rock pressure is the **k-factor**, which, all other things being equal, increases with increasing setting pressure and decreasing medium modulus (Su and Hasenfus, 1990).

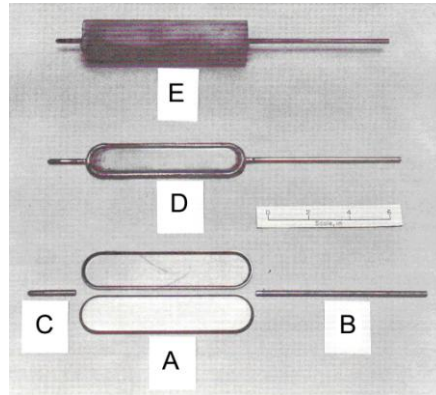


**Fig. 11.3.17 BPC and components: A is steel platen, B and C are stainless steel tubing used to pressurize the BPC, D is completed flat jack, and E is the grout-encapsulated BPC (Haramy and Kneisley, 1991)**

The cylindrical borehole pressure cell (CPC) measures radial pressure changes in the materials surrounding the borehole in which it is installed. It cannot distinguish between vertical and horizontal pressures. The CPC consists of a copper shell (Fig. 11.3.18B) brazed to a steel core (Fig. 11.3.18A). The cell diameter is 1.49 in. (37.85 mm) for installation in a borehole 1.5 in. (38.1 mm) in diameter. It is 8 in. (203.2 mm) long. Hydraulic fluid is pumped into the annulus between the steel core and copper shell which is then expanded against the hole wall.

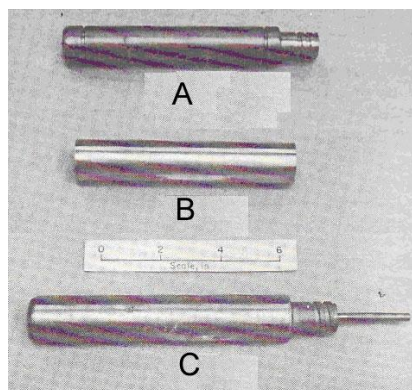


**Fig. 11.3.18 Cylindrical pressure cell (CPC) and components: A, steel core, B, copper shell, and C, completed CPC (Haramy and Kneisley, 1991)**

CPC and BPC can be installed together in a borehole or installed separately for measurement of stress changes or stresses. For CPC, various methods have been developed for calculating the stress changes and stresses in the surrounding rock (Babcock, 1986; Lu, 1984 and 1985).

The CPC measures the radial stress changes around the borehole wall, assuming the radial pressure is uniformly distributed, then

For plane stress condition

$$\Delta\sigma_v + \Delta\sigma_h = \frac{\Delta P_{cpc} C_s E}{2\pi a^2 L} \tag{11.3.32}$$

For plane strain condition

$$\Delta\sigma_v + \Delta\sigma_h = \frac{\Delta P_{cpc} C_s E}{2\pi a^2 L(1-\nu^2)} \tag{11.3.33}$$

where  $\sigma_v$  and  $\sigma_h$  are vertical and horizontal stresses, respectively,  $\Delta P_{cpc}$  is observed CPC pressure change,  $E$  is Young's modulus of rock,  $L$  is CPC length,  $a$  is borehole radius,  $\nu$  is Poisson's ratio of rock, and  $C_s$  is cell and system stiffness from the expansion test.

Vertical or horizontal stress changes can be determined by the BPCs, depending on whether the BPC is oriented vertically or horizontally, because a BPC measures only the stress perpendicular to it.

For plane stress condition

$$\Delta\sigma_v = \frac{\Delta P_{cpc} C_s E}{2\pi a^2 L} \tag{11.3.34}$$

For plane strain condition

$$\Delta\sigma_v = \frac{\Delta P_{cpc} C_s E}{2\pi a^2 L(1-\nu^2)} \tag{11.3.35}$$

In-situ rock stresses are calculated from either a three-cell package (one CPC and two orthogonally oriented BPCs) (Fig. 11.3.19), or, if the local rock response ratio is known, a two-BPC package (Lu, 1986).

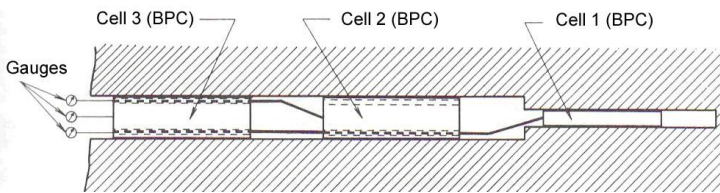


Fig. 11.3.19 Schematic of three-cell installation (Haramy and Kneisley, 1991)

**A. For three-cell installation**

$$Q = \frac{P_{e-bph}}{P_{e-bpv}} \tag{11.3.36}$$

$$\sigma_v + \sigma_h = \frac{P_{e-cpc}}{(1-\nu)} \quad (11.3.37)$$

$$\frac{\sigma_h}{\sigma_v} = \frac{Q - S_c}{1 - QS_c} \quad (11.3.38)$$

where  $P_{e-bph}$ ,  $P_{e-bpv}$ , and  $P_{e-cpc}$  are horizontal, vertical, and radial pressure cell readings for BPC and CPC, respectively,  $S_c = 0.185$  is BPC transverse sensitivity.

### B. When the rock response ratio is known

The **response ratio** of rock is defined as

$$K = \frac{P_{e-cpc} - P_{e-bpv}}{\sigma_h + S_c \sigma_v} \quad (11.3.39)$$

or 
$$K = \frac{P_{e-cpc} - P_{e-bph}}{S_c \sigma_h + \sigma_v} \quad (11.3.40)$$

$$\sigma_v = \frac{P_{bpv} - S_c P_{bph}}{K(1 - S_c^2)} \quad (11.3.41)$$

$$\sigma_h = \frac{P_{bph} - S_c P_{bpv}}{K(1 - S_c^2)} \quad (11.3.42)$$

### 3. Biaxial Stress Meter

A biaxial stress meter measures the principal stress changes in a plane perpendicular to the borehole. Its arrangement of sensing elements is similar to the three-component borehole deformation gauge in that three diametrical vibrating wires are mounted at 120° intervals around the circumference of a cylinder (Fig.11.3.20). Changes of stress cause corresponding changes in wire length, which, in turn, exhibits changes in resonant frequency of vibration of the sensor.



Fig. 11.3.20 Biaxial stress meter (Courtesy Geokon Inc.)

The magnitude and orientation of the principal stresses are determined from the measured radial deformation of the vibrating wires in three directions (Geokon, 2004),

$$U_{r1} = A(\sigma_1 + \sigma_2) + B(\sigma_1 - \sigma_2) \cos 2\theta_1 \quad (11.3.43)$$

$$U_{r2} = A(\sigma_1 + \sigma_3) + B(\sigma_1 - \sigma_3)\cos 2\theta_2 \quad (11.3.44)$$

$$U_{r3} = A(\sigma_2 + \sigma_3) + B(\sigma_2 - \sigma_3)\cos 2\theta_3 \quad (11.3.45)$$

where  $U_{r1}$ ,  $U_{r2}$ , and  $U_{r3}$  are radial deformation for vibrating wire oriented at  $\theta_1$ ,  $\theta_2$ , and  $\theta_3$  directions.  $\theta_1$  is the angle, measuring clockwise, from  $\sigma_1$  to vibrating wire oriented at  $\theta_1$  direction, and

$$A = \frac{R_2}{8G} \left[ C_2(X_s - I)\frac{R_c}{R_2} + C_5\frac{R_2}{R_c} \right] \quad (11.3.46)$$

$$B = \frac{R_2}{8G} \left[ C_3(X_s - 3)\frac{R_c^3}{R_2^3} + C_7\frac{R_c}{R_2} + C_1(X_s + I)\frac{R_2}{R_c} + C_4\frac{R_2^3}{R_c^3} \right] \quad (11.3.47)$$

$$\theta_2 = \theta_1 + 60^\circ \quad (11.3.48)$$

$$\theta_3 = \theta_1 + 120^\circ \quad (11.3.49)$$

where  $C_1$  through  $C_7$  are coefficients dependent on the stress meter geometry and the material properties of the stress meter and rock,  $2R_c = 1$  in. (25.4 mm) is the length of the vibrating wire, subscripts  $s$  and  $i$  denote the material properties of the stressmeter and surrounding rock, respectively.

$$G = \frac{E}{2(I + \nu)} \quad (11.3.50)$$

$$X = \frac{3 - \nu}{1 + \nu} \quad \text{for plane stress} \quad (11.3.51)$$

$$X = 3 - 4\nu \quad \text{for plane strain} \quad (11.3.52)$$

Solving for  $\sigma_1$ ,  $\sigma_2$ , and  $\theta_1$  from Equations 11.3.43 through 11.3.45,

$$\sigma_1 = \frac{1}{2} \left\{ \frac{1}{3B} \left[ (2U_{r1} - U_{r2} - U_{r3})^2 + 3(U_{r2} - U_{r3})^2 \right]^{\frac{1}{2}} + \frac{1}{3A} (U_{r1} + U_{r2} + U_{r3}) \right\} \quad (11.3.53)$$

$$\sigma_2 = \left[ \frac{1}{3A} (U_{r1} + U_{r2} + U_{r3}) - \sigma_1 \right] \quad (11.3.54)$$

$$\theta_1 = \frac{1}{2} \cos^{-1} \left[ \frac{U_{r1} - A(\sigma_1 + \sigma_2)}{B(\sigma_1 - \sigma_2)} \right] \quad (11.3.55)$$

But because  $\cos \theta = \cos(-\theta)$ , Equation 11.3.55 has two solutions.

$$\text{If } U_{r2} = A(\sigma_1 + \sigma_2) + (\sigma_1 - \sigma_2)\cos 2(\theta_1 + 60^\circ), \text{ then } \theta_1 \text{ is positive.} \quad (11.3.56)$$

$$\text{If } U_{r2} = A(\sigma_1 + \sigma_2) + (\sigma_1 - \sigma_2)\cos 2(\theta_1 + 120^\circ), \text{ then } \theta_1 \text{ is negative.} \quad (11.3.57)$$

## 11.4 DEFORMATION-MEASURING DEVICES

Deformation in underground coal mines mainly refers to convergence between the floor and roof of entries or faces where excessive convergence during their useful lifetime can reduce headroom and make it difficult to move machinery and carry out mining operations. Excessive convergence is due to either extremely heavy pressure or insufficient support or weak roof and/or floor strata. Another type of deformation is bed separation or differential strata sag in the immediate roof. The devices used to detect the roof-to-floor deformation can also be used to detect the depth of floor heave or differential heaving in the floor strata.

### 11.4.1 Convergence Meters

Of course conventional rulers and tapes can be used to measure convergence between the floor and roof of the entries, but they usually do not have enough sensitivity to detect the onset of convergence. Therefore, deformation is generally measured with a convergence meter, which is a rod of adjustable length, with a dial gauge, or a vernier scale, or a micrometer, or a LVDT (linear variable distance transformer) attached at one end (Fig. 11.4.1).

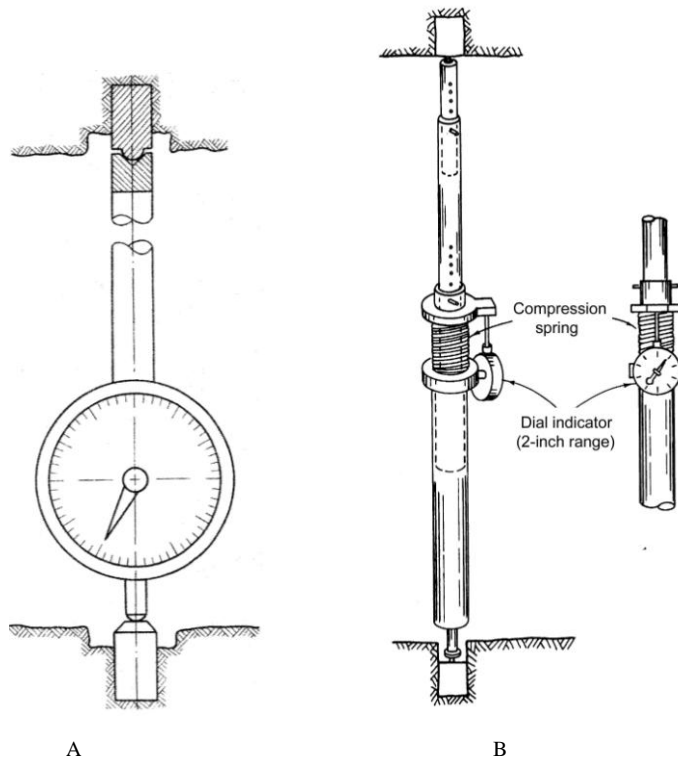


Fig. 11.4.1 Two examples of convergence meters

To establish a convergence station, an anchor is inserted in a hole drilled at least 6 in. (152.4 mm) into the roof and floor. The anchors in the roof and floor must be located in the same vertical plane. The anchors in the roof and floor must be recessed, and the top end of the anchors should not project beyond the roof or floor line. Different types of anchors have been used. Expansion-shell roof bolts can be anchored directly at the bottom of the hole, whereas

straight metal rods have to be grouted. When a reading is to be made, the length of the convergence meter is adjusted to approximately the distance between the roof and floor anchors. Once this is done, a reading is made from the dial gauge. To avoid any subsequent confusion, the dial gauge readings are combined with the length of the rod to obtain the total distance between the roof and floor anchors. Any subsequent reading will indicate any change in distance. To facilitate the insertion of the convergence meter on the anchors, the end of the anchors where connections are made are either hemispherical or conical, so they will fit intimately with the conical or hemispherical end of the convergence meter.

The ultrasonic convergence instrument consists of a Polaroid sonar transducer and auto-ranging system for precise distance measurement (Fig. 11.4.2) (McVey, 1984). An oscillator generates a wave that causes the sonar transducer to emit a signal every 6 second. The signal, on hitting an object, will be reflected back to the transducer. The round-trip travel time, i.e., the time required for the emitted signal to reach the object and return to the transducer, is accurately timed and converted into feet and displayed digitally. The rate of convergence is determined by finding the difference in distance between two consecutive signals which are emitted in 6-sec intervals. The instrument can measure convergence from 1 to 35 ft (0.3 to 10.7 m) with 0.001 ft (0.3 mm) resolution and rate of convergence from 0.01 to 35 ft (0.03 to 10.7 m) per minute. It can be monitored remotely and equipped with an alarm that will be set off once the preset rate of convergence is exceeded.



**Fig. 11.4.2 Ultrasonic convergence instrument (McVey, 1984)**

The mechanical convergence instrument consists of two telescoping potentiometer convergence meters and a digital readout control box (Fig. 11.4.3) (McVey and Howie, 1981). The convergence meter can accommodate an opening height from 4.5 to 12 ft (1.4 to 3.7 m) with a 6 in. (152.4 mm) measuring range. Convergence is sampled every 10 seconds for 10 milliseconds. The samples in two consecutive samplings are compared, and the difference is converted and displayed as rate in inches per minute. The instrument has a maximum measurement range of 6 in. (152.4 mm) with an accuracy of 1 %. It can measure rate of convergence from 0 to 6 in. (0 to 152.4 mm) per minute. The instrument is monitored remotely and can be equipped with an alarm off by a preset rate of convergence ranging from 0 to 1 in. (0 to 25.4 mm) per minute. It has been successfully used to predict impending roof caving in room-and-pillar retreating operations (McVey and Howie, 1981).



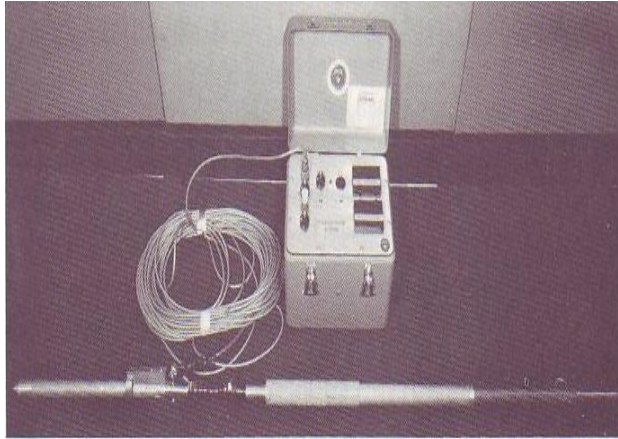


**Fig. 11.4.3 Mechanical convergence instrument (McVey and Howie, 1981)**

The tape extensometer (Fig. 11.4.4) consists of a steel tape, a compression spring, a dial gauge, and a tensioning screw. During installation, the tape is extended to the nearest perforated hole and locked. The top end is hooked to the roof anchor, and the bottom hook of the extensometer is attached to the floor anchor. The tensioning screw is turned to adjust the applied tension. The correct tension is obtained when the marker lines match in the correct tension indicator. At this time the dial gauge is read. The difference in the two consecutive readings at a predetermined interval is the convergence between the two anchors. When the convergence exceeds the 2 in. (50.8 mm) stroke or the dial gauge, the tape is extended 2 in. (50.8 mm) to the next perforated hole.

The sonic probe convergence meter (Fig. 11.4.5) consists of two telescoping tubes and a built-in sonic probe. A ring magnet is attached to the inner side of each tube. The distance between the two ring magnets is measured by a sonic probe. The sonic probe is composed of a probe head and a rigid tube of magnetostrictive material. When a pulse is sent from the readout meter to the probe, it generates an instantaneous magnetic field along the length of the probe. A sudden discontinuity in magnetic field will be formed at the point where each ring magnet is located. This creates a stress wave that travels to the probe head and actuates an oscillator. The oscillator then times the arrival of the pulse for the second magnet. The distance between the first and second magnet position is displayed on the readout meter. The distance difference between the two magnets in any two readings is the roof-to-floor convergence.

The wire pull displacement transducer is a ratiometric potentiometer (voltage divider) (Fig. 11.4.6) that converts the string extension into a voltage proportional to the displacement of the string. It comes in various sizes (displacement range) and accuracy. For convergence measurements, the transducer is hooked up to a permissible data logger that provides the excitation voltage and records the output voltage as the convergence develops (Barczak et al., 2008).

It must be emphasized that if the entries/crosscuts are being used for traveling, continuous monitoring of roof to floor convergence may not be feasible using devices that require stretching from roof to floor. Constant traffic requires that the roof and floor anchors must be recessed inside the hole. Alternatively, a sonic transducer mounted on the roof is recommended. The sonic wave emitted from the transducer travels and is reflected from the floor. The time interval between emission and receiving can be used to measure the convergence (Dunford and Serbousek, 1993).

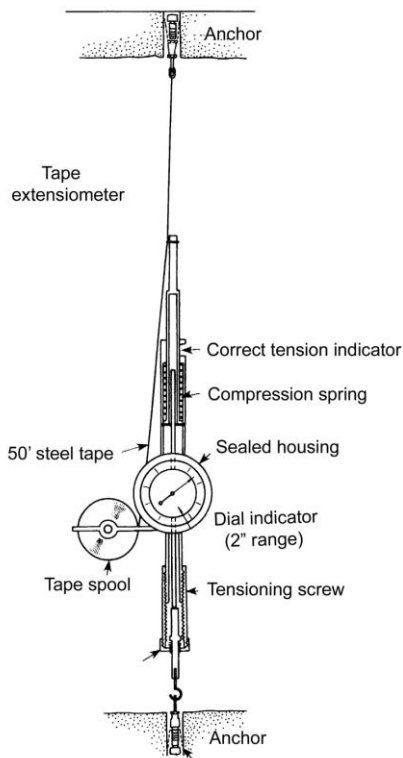


Fig. 11.4.4 Tape extensometer

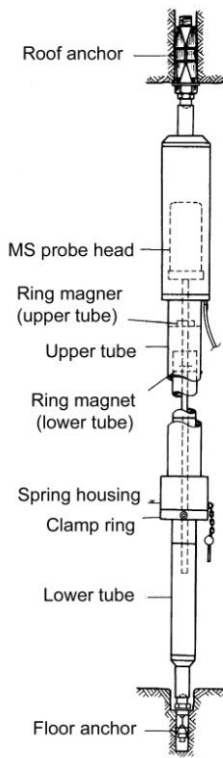


Fig. 11.4.5 Sonic probe convergence meter



Fig. 11.4.6 Ratiometric potentiometer (Barczak et al., 2008)

### 11.4.2 Differential Roof Sag Meters

Differential roof sag measuring devices measure the difference in roof sag at various horizons in the roof as an indication of roof stability. Generally speaking, if there is a differential roof sag between two horizons, it may represent the occurrence of bedding separations or fractures. The multiple-position extensometer is designed for this purpose. The key to this device is to have anchors attached to various horizons and measure movement and compare between any

two anchors for differences to identify the location and amount of movement. There are many types of anchors including springs, wedges, expansion shells, grouting, or hydraulic pressure.

A roof sag extensometer that is the simplest, yet accurate enough for most purposes uses high strength U-shaped pins as anchors (Fig. 11.4.7A). It can be set as follows: an upright U-pin is squeezed slightly into a short tube with a smaller diameter than the borehole. The short tube is then lifted to the position where anchorage is intended. The pin in the tube is pushed out of the short tube and sprung against the wall of the borehole to anchor. A rod or string is dropped from the pin to the collar of the hole. The distance between the rod at the hole collar and an anchor on the floor is monitored by a dial gauge attached with a fixed-length string. Any stratum sagging is accompanied by downward movement of the pin attached to that stratum and thus induces changes in the dial gauge readings. Several pins can be installed similarly in the same hole to detect differential strata movement. In Fig. 11.4.7B, the anchors are made of reverse U-pins.

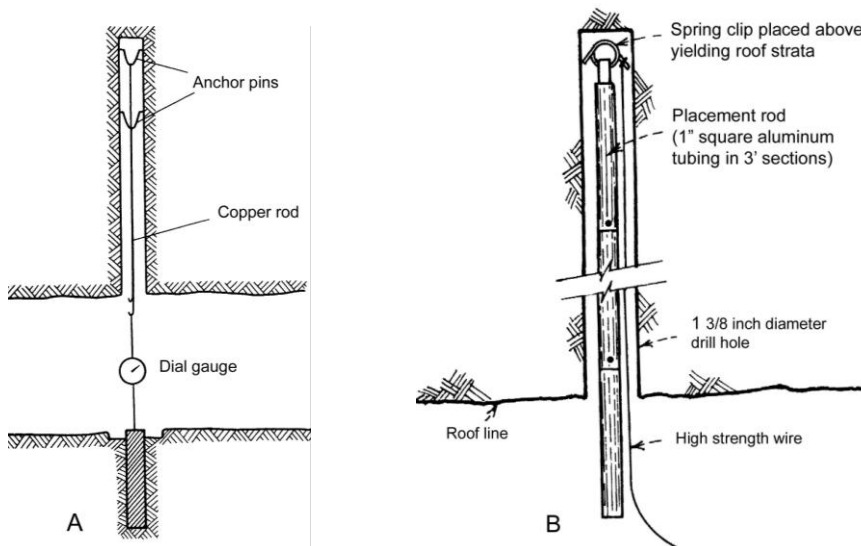


Fig. 11.4.7 A, U-pin roof sag meter (Peng and Park, 1977b); B, Coil-type roof sag meter (Radcliff and FitzSimmons, 1977)

The single-position rod extensometer (Fig. 11.4.8A) uses two expansion-shell rock-bolt anchors set by a socket wrench, one at the horizon deep into the borehole and the other at the collar. The deep anchor has a thin rod that extends beyond the bottom hole in the collar anchor. A depth micrometer is used to measure the amount of rod extension against the bottom surface of the collar anchor. The difference in two subsequent readings is indicative of the movement of the top anchor. In the double-position rod extensometer, two top anchors are attached at different horizons, and each has a thin rod to extend beyond a separate hole in the collar anchor (Fig. 11.4.8B). Figure 11.4.8C shows a triple-position rod extensometer with snap ring anchors. The anchor is installed by pushing it to the desired horizon and pulling a cord to remove the locking pins. This allows the retaining rings to expand against the wall of the borehole and retain the anchor. Each anchor has a thin rod that extends freely through lower anchors and terminates inside a hole in the collar anchor. A depth micrometer is used to measure the location of the rod tip from each anchor. A maximum of eight anchors can be installed in a borehole 3 in. (76.2 mm) in diameter and up to 150 ft (45.7 m) deep.

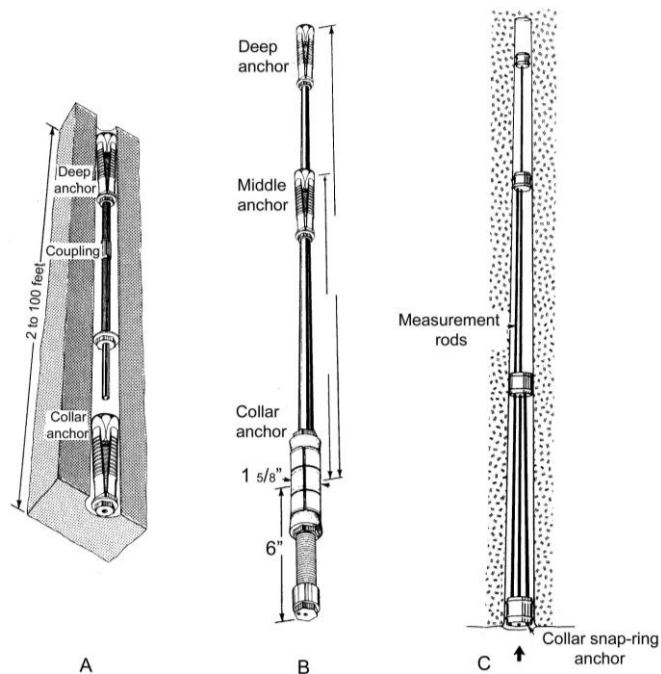


Fig. 11.4.8 Single- A, double- B, and triple- C, extensometer

The sonic probe system has also been developed and used extensively for monitoring the differential roof sag in underground coal mine roofs (Fig. 11.4.9). The system consists of a flexible sonic probe, a sonic probe read-out box, a black plastic guide tube with dummy top anchor attached, and a string of extensometer magnetic anchors. The installation procedure is as follows: drill a hole in the roof 2-1/6 in. (55 mm) in diameter by 26 ft (8 m) long. Insert the black plastic guide tube into the hole using the installation rods, making sure the top anchor are pushed to the back of the hole or approximately the 25 ft (7.7 m) mark. The magnetic anchors are then pushed onto the black guide tube to the desired positions, one each time, sequentially from the top down. The bottom anchor is doubled and is installed approximately 1 in. (25.4 mm) past the collar of the hole. A maximum of 20 anchors can be installed in a borehole (Geokon, 1995).

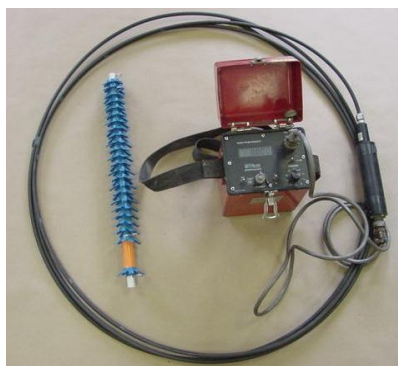


Fig. 11.4.9 Sonic roof extensometer system

A sonic probe can detect movement as small as 0.04 in. (1 mm). The measured displacement profiles along the borehole can be used to identify the location of a weak zone and bed separations or cracks (Whittaker and Frith, 1987). Figs. 11.4.10 and 11.4.11 show two examples of roof extensometry data. In Fig. 11.4.10, roof displacement was restricted to approximately 6.6 ft (2 m) high, within which the immediate roof 2 ft (0.6 m) thick might have been separated. In Fig. 11.4.11, the roof displacement reached 15.7 ft (4.8 m) high. The 8 ft (2.4 m) bolts could not stop roof movement. Conversely, the 12 ft (3.65 m) cable bolts were quite effective in restraining roof movement.

The telltale system is a visual device exhibiting the level of roof movement by color code. In this system, one to three anchors are normally used, and they are referred to as single, dual and triple height telltale systems (Fig. 11.4.12) (Bigby and DeMarco, 2001). Each anchor has a wire, the bottom end of which is attached to a column with three color bands, each 1 in. (25 mm) long. The downward movement of the anchor, and thus the roof strata, can be visually estimated by the length of each color band protruding from the reference tube, or top indicator, or from the roof line. Each color code represents a level of roof movement and can be used as an action level, depending on site-specific conditions. The top indicator (A) should be anchored 1 ft (0.3 m) below the top of the bolt, as this region cannot be deemed to be fully reinforced.

All indicators are concentric design, i.e., C indicator slides inside B indicator, which in turn slides inside A indicator. This means that in the dual telltale system, the A indicator can directly shows deformation within the bolted height, and the B indicator directly shows deformation above the bolted height without the need for calculation by the observers. The telltale units can be monitored remotely (Bigby et al., 2003 and 2006).

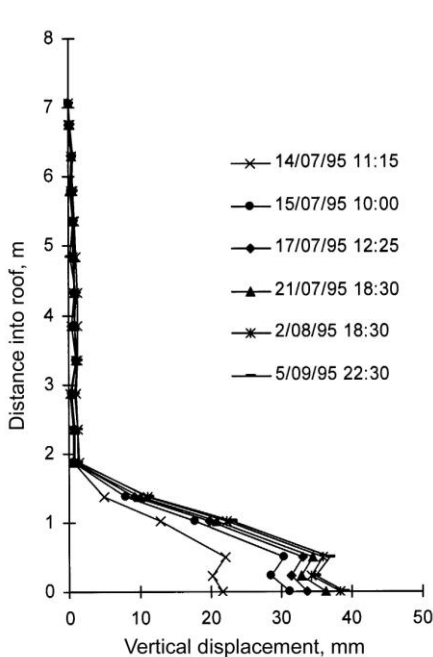


Fig. 11.4.10 Roof extensometry data from an Australia coal mine (Frith and Colwell (2006)

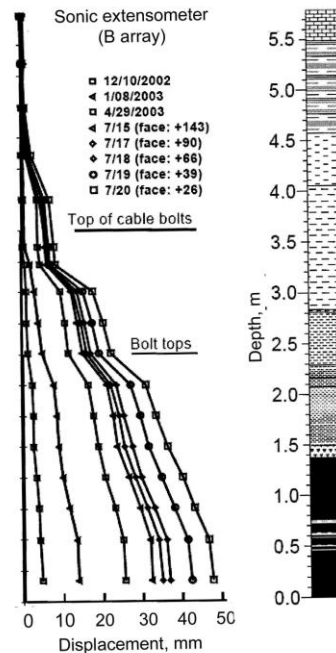


Fig. 11.4.11 Roof extensometer data from a U.S. coal mine (Oyler et al., 2004)

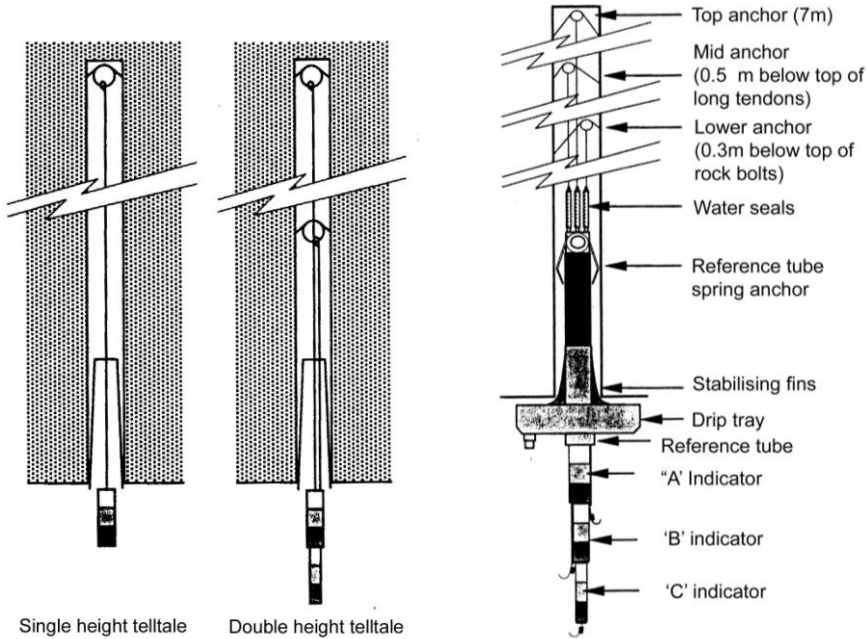


Fig. 11.4.12 Telltale systems (Bigby and DeMarco, 2001; Bigby et al., 2003)

**11.5 STRAIN-MEASURING DEVICES**

Among the various strain-measuring devices available, strain gauges are the most widely used. However, in underground coal mine instrumentation, strain gauges are generally used indirectly, in contrast to the strain measurement of a laboratory specimen where they are mounted directly on the surface of the specimen. For example, in a three-component borehole deformation gauge (p. 514), strain gauges are attached and used to monitor the deflection of the cantilever beams caused by the changes in borehole diameters.

An electrical resistance strain gauge (Fig. 11.5.1A) consists of a grid of thin wires cemented on a paper of Bakelite backing or a metallic foil grid deposited on a plastic film. When a strain gauge is properly mounted on a surface, any strain induced on the surface will be completely transmitted to the strain gauge. The principle of strain gauging is that whenever a wire is compressed due to a compression to the surface to which it is attached, its cross-sectional area increases and electrical resistance decreases and vice versa. The change in resistance per unit resistance is proportional to the change in length per unit length (i.e., strain) or

$$\frac{\Delta R}{R} = G \frac{\Delta L}{L} \tag{11.5.1}$$

where  $R$  is resistance,  $\Delta R$  is change in resistance,  $L$  is gauge length,  $\Delta L$  is change in gauge length, and  $G$  is the gauge factor and usually runs in the neighborhood of 2.

To measure the strain gauge output, it is necessary to wire the active gauges in a Wheatstone bridge circuit (see Fig. 11.2.2, p. 509), The strain indicator with a built-in Wheatstone bridge circuit (Fig. 11.5.1B) is designed specifically for this purpose. The amount

of strain can be read directly from the digital display of a strain indicator once the bridge circuit is properly balanced. Alternatively, the measured strain is digitized and recorded directly onto a computer for analysis.

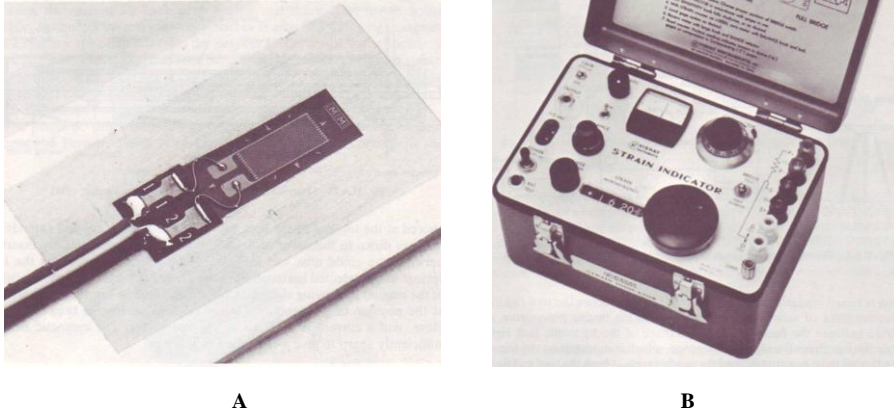


Fig. 11.5.1 A, strain gauge B, strain indicator (Peng, 1986)

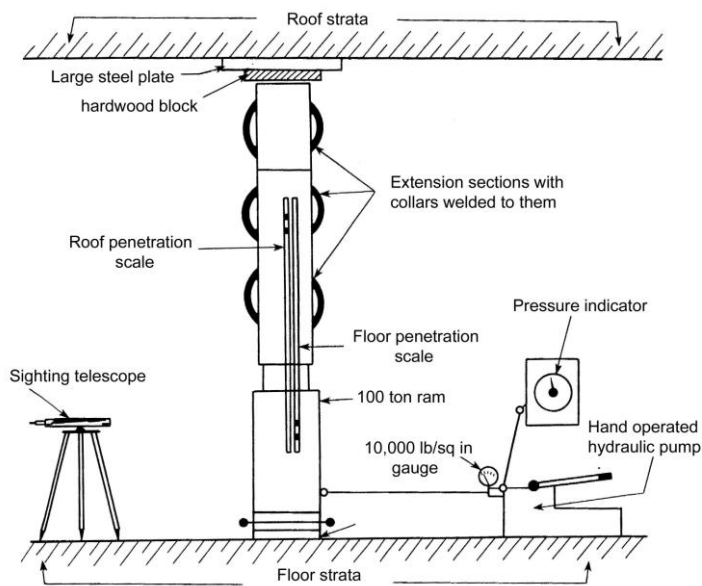
The resistance of metal is temperature dependent, i.e., a change in temperature will create strains measurable by a strain gauge. Therefore temperature-compensating gauges are usually placed on the arms of the bridge circuit to eliminate the temperature-induced strain.

Depending on the purpose of the application, various types and sizes and lengths of strain gauges are available, including embedment strain gauges for the measurement of dynamic strains, weldable strain gauges for welding to steel structures, and fiber optic strain gauges for use in environments where conventional strain gauges are not suitable.

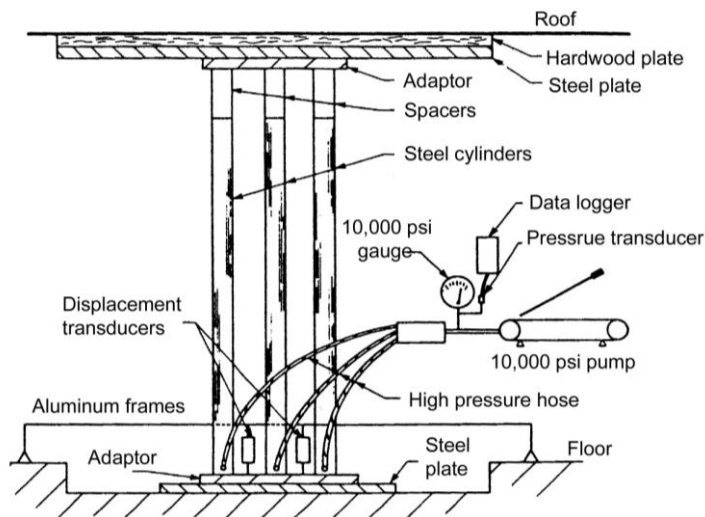
## 11.6 BEARING CAPACITY OF THE ROOF AND FLOOR

The bearing capacity of the roof and floor is determined by the bearing capacity test (Fig. 11.6.1) (Conroy and Curth, 1981). The testing apparatus consists of a 100-ton hydraulic ram, extension sections, a sighting telescope, and a hand pump. During testing, the hydraulic ram is set up on the floor at the location where the roof or floor bearing capacity is to be measured. If the floor bearing capacity is to be determined, a thick square hardwood block and steel plate at least four and two times, respectively, larger in area than that of the cross-section area of the cylinder of the hydraulic ram should be inserted in that order between the hydraulic ram and the roof. This procedure reduces pressure on the roof. On top of the ram piston, three extension sections are added to reach a height approximately 6-12 in. (152.4 – 304.8 mm) from the roof line. The extension sections with a detachable collar are inserted. The piston is raised gradually until the hardwood block touches the roof tightly. A bearing plate of variable size, depending on the testing procedures, is inserted between the floor and bottom surface of the hydraulic jack right before testing. From the sighting telescope, which is mounted on the tripod and adjusted to be horizontal, the height levels are read at both the roof and floor penetration scales. These are the zero readings. Loads are applied gradually by operating the hand pump,

and the penetration scales are read at fixed load increments until the floor fails. The ultimate load at which the floor fails divided by the area of the bearing plate is the bearing capacity of the floor for that plate size (Barry and Nair, 1970).



A



B

**Fig. 11.6.1 Bearing capacity test apparatus: A, adapted from Conroy and Curth (1981)  
B, used by Su et al., (1993)**

If the roof bearing capacity is to be determined, the hardwood blocks and the large steel plate must be inserted between the floor and the extension sections and the bearing plate inserted directly between the roof and the adaptor beneath the ram cylinder.



Figure 11.6.2 shows an example of the floor bearing capacity test results for selection of the best floor horizon for longwall mining. Horizon 1 (silicious shale) and 2 (medium-hard claystone) are not suitable for a panel floor due to their low bearing capacities. Horizon 3 (hard shale) would be an excellent floor. But if horizon 3 is chosen, a dirt band of 14 in. (355.6 mm) will have to be cut out with the coal, which will dilute the quality of the run-of-mine coal.

The ultimate bearing capacity determined by the test apparatus shown in Fig. 11.6.1 is a function of the size of the bearing plate. In fact the ultimate bearing capacity decreases with the increase in plate size (Fig. 11.6.3). Yu et al., (1993) suggested a reduction of 0.23-0.25 for those determined by using an 8 in. (203.4 mm) plate size. Therefore, the bearing capacity varies with the size and shape of the bearing plate, a series of plate sizes and shapes must be used in order to obtain the bearing capacity of the floor.

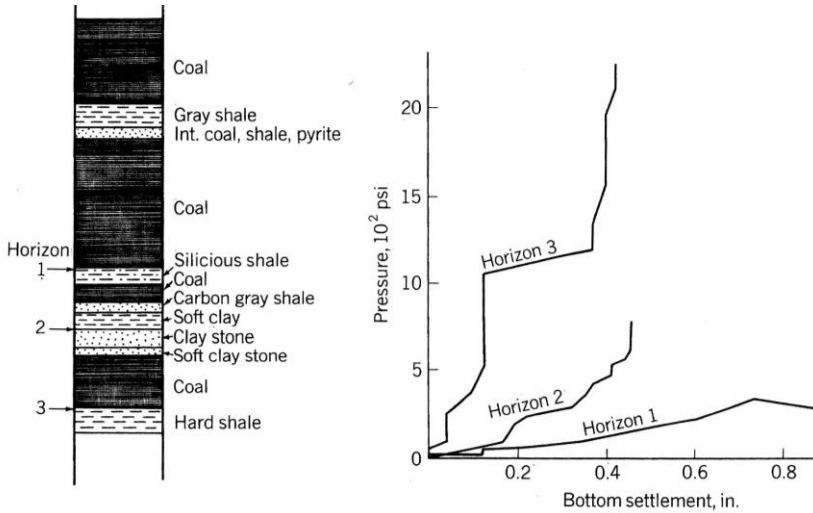


Fig. 11.6.2 Method of selecting the best floor horizon by the floor bearing capacity test

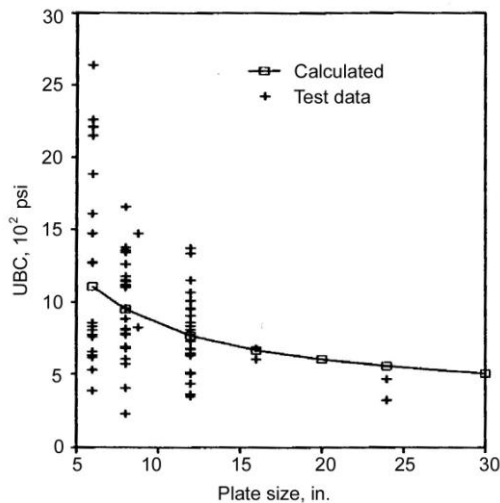


Fig. 11.6.3 Measured ultimate bearing capacity (UBC) of floor (Yu et al., 1993)

## 11.7 BOREHOLE OBSERVATION DEVICES

The stratoscope or borescope has long been used for inspection of roof strata conditions inside a borehole (FitzSimmons et al., 1979; Herget, 1982; Lenox, 1980).

The fiberoptic stratoscope consists of three components (Fig. 11.7.1) (FitzSimmons et al., 1979): the flexible section, eyepiece assembly, and object end. The flexible section is made of four bundles of optic fibers. The largest bundle in the center is for image viewing, and the three smaller bundles surrounding the central image bundle are for transmitting light to the object end for viewing. The object end has a right-angle mirror that allows a 40° field of view of the wall of the borehole. The fiberoptic stratoscope is 0.75 in. (19 mm) in diameter for a one inch (25.4 mm) drill hole. The flexible length is 101 in. (2.57 m) long. Its minimum bending radius is 5 in. (127 mm). Thus, it is extremely flexible and can be carried with ease.



Fig. 11.7.1 Fiberoptic unit (FitzSimmons et al., 1979)

The latest development in borescope technology is to incorporate a video camera for viewing and recording (Anderson and Prosser, 2007; Peng and Sasaoka, 2005; Unrug, 1994). It generally consists of three parts: the probe where the camera is located, a monitor, and installation rods (Fig. 11.7.2). The scanned images are recorded on a CD for detailed viewing and analysis (Fig. 11.7.3).



Fig. 11.7.2 FLETCHER borescope (Anderson and Prosser, 2007)

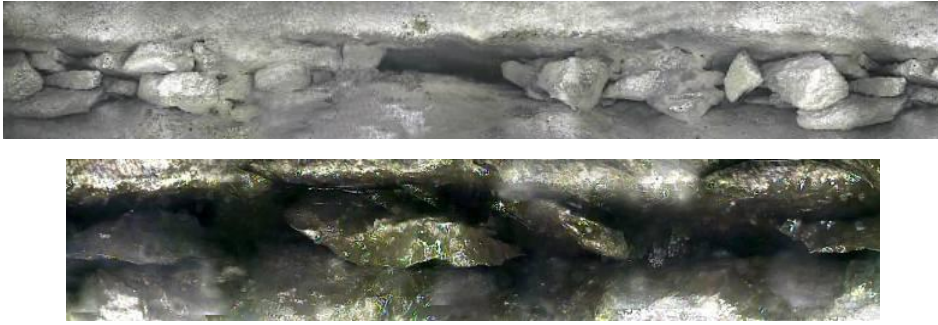


Fig. 11.7.3 Voids, 0.75 in. (19 mm) thick as observed from borescope video (Anderson and Prosser, 2007)

## 11.8 OVERBURDEN STRATA MOVEMENT MONITORING DEVICES

Overburden strata movement monitoring devices track the progression of strata disturbance in the overlying strata as the longwall face or retreat pillar line advances. They are normally installed in surface boreholes with an NX-sized core (2-1/8 in. or 54 mm) or larger. The boreholes are drilled from the surface all the way down to the coal seam or some distance above the coal seam to be mined. Movement of strata at different horizons above the coal seam is then monitored from the surface as a function of face location. Most devices in this category are designed to measure vertical displacement; only one device can measure both vertical and horizontal displacement (Peng, 1992).

One major problem with overburden strata movement monitoring using surface boreholes is that the boreholes are often blocked off partially or completely during the monitoring period. This is due to the mining-induced lateral strata movement along the bedding planes.

### 11.8.1 Wireline Bullet Perforations

This technique makes use of electronic logging devices commonly used in oilfields. One conventional well completion technique is bullet perforation. The bullet perforator is essentially a multi-barreled firearm that is designed to be lowered into a well, positioned at the desired level, and electrically fire a bullet into the wall of the well by means of a surface control. Depending on the design of the bullets or projectiles, the depth of penetration through the casing and cement and into the surrounding strata varies. If an encapsulated cobalt wire is inserted in the bullet, when the bullet is shot into the stratum surrounding the borehole and remains there, stratum movement can be followed. A borehole drilled for subsidence monitoring is usually not cased, and bullets are shot directly into various strata along the borehole. Their positions are identified with high peaks of radioactive intensity in a gamma ray log. The change in a bullet's location indicates the amount and direction of movement (usually downward in a subsidence study) of a stratum in which the bullet is inserted. Frequency of logging depends on face location. When the face is closer to the borehole, the bullet's position should be logged more frequently, because greater and faster ground movement is expected.

### 11.8.2 Time Domain Reflectometry (TDR)

Time domain reflectometry or TDR works on the same principle as radar. A good coaxial cable is grouted in the borehole all the way down to the coal seam. Caving or separation of the roof strata shear off and create some sort of "faults" in the coaxial cable. When a voltage step of ultrafast rise time is sent down the cable, each coaxial cable fault will reflect the incoming

signal and cause energy to travel back toward the cable input where a sampler picks up the voltage and superimposes it on the advancing initial step. The summation will result in a step up or step down transition on the CRT (cathode ray tube or oscilloscope) display depending on whether it is reflected in phase or out of phase with respect to the initial step.

Basically, TDR depends on a disturbance in cable impedance to “see” a fault. Impedance ( $Z$ ) is the product of cable resistance and signal speed. It can be related to the signal reflection coefficient  $P$  by

$$Z = 50 \left[ \frac{1 + P}{1 - P} \right] \tag{11.8.1}$$

where  $P$  is the ratio of incoming initial voltage  $E+$  to the reflected voltage  $E-$  and assumes a value between - 1 and + 1. A rise on the display indicates a positive  $P$ , the maximum of which (i.e., + 1) is caused by an open-circuit cable fault, whereas a dip results from a negative  $P$ , the maximum of which (i.e., - 1) is from a short-circuited cable fault. Any value between + 1 and - 1 corresponds to a type of cable fault that can be calibrated in the laboratory.

Figure 11.8.1 shows a method of installing a TDR coaxial cable in the borehole (Dowding et al., 1986). The bottom end of the coaxial cable is attached to an anchor and sealed against water seepage. As the coaxial cable is lowered gradually into the borehole, it is firmly crimped at desired spacing to provide reference reflection signals. The cable is grouted into the wall rock of the borehole with an expansive cement grout.

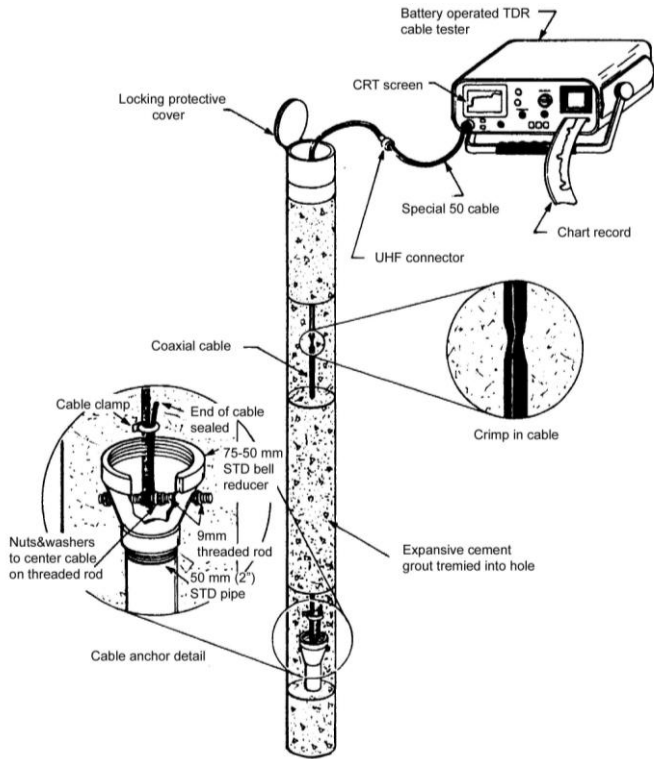


Fig. 11.8.1 Details of TDR installation (Dowding et al., 1986)

In general, TDR cable failures occurred at strong-to-weak rock interfaces and in weak strata such as claystone and coal seams. Near surface responses correlated well with interfaces between sandstone beds and weaker strata. Propagation of TDR failure ceased upon passing of the traveling subsidence tensile wave (Su and Hasenfuls, 1987; Hasenfuls et al., 1988).

### 11.8.3 Multi-position Borehole Extensometer (MPBX)

An MPBX is a specially constructed instrument that measures the differential vertical movement of selected rock horizons in a borehole relative to the surface.

Figure 11.8.2 shows a setup of an MPBX used to monitor overburden deformation (Ingram and Trevits, 1992; Khair et al., 1987a; Whittaker and Frith, 1987). The surface borehole was 8-5/8 in. (219 mm) in diameter. Each MPBX unit consists of 8 steel cables tied to 8 hardened steel, spring-loaded anchoring mechanisms. Each anchor is attached to the walls of the borehole by friction at a pre-determined rock horizon. The steel cable is then extended from the anchor to the surface where they are attached to a common counter-weight surface head assembly. To prevent tangling, each cable is slipped through thin plastic tubing filled with hydraulic fluid. This tubing protects the cables from contacting and being glued to the grout/bentonite mixture that is used to backfill the borehole after the installation of anchors has been completed. The head assembly consists of a reference depth gauge for mechanical readings and linear potentiometer (LVDT) for remote reading. The displacement of each anchor is recorded by a data logger at pre-set intervals. These data are used to analyze the movement of and differential movements between anchors. In case of data logger failure, manual measurement at the head assembly can be performed.

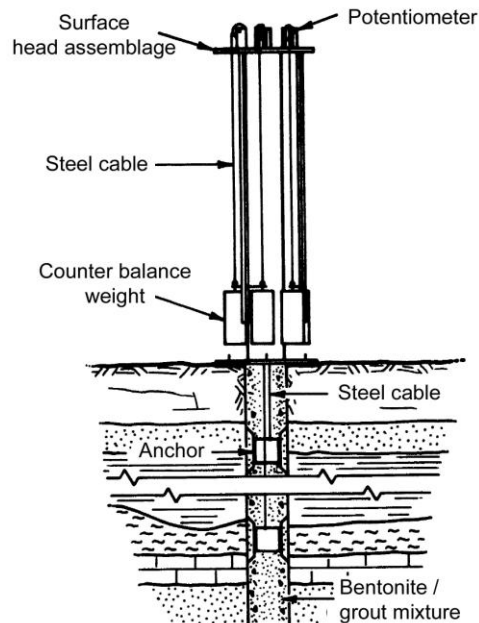


Fig. 11.8.2 Schematic of Multi-position Borehole Extensometer (MPBX) (Ingram and Trevits, 1992)

Figure 11.8.3 shows anchor displacement development curves obtained from a mechanical grouted assembly (Khair et al., 1987a). Note that the strata above anchor 5 moved

in unison, indicating no strata separation. A very large separation occurred between anchors 4 and 5. Similarly a large separation occurred between anchors 2 and 3.

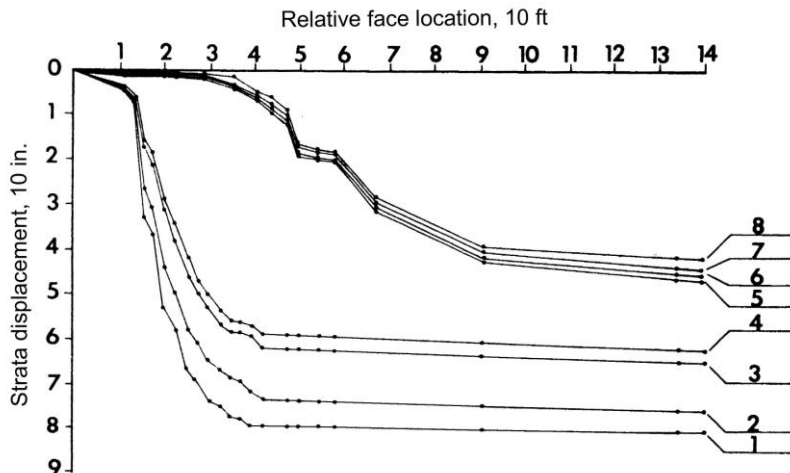


Fig. 11.8.3 MPBX anchor displacement development curves (Khair et al., 1987a)

The full profile borehole extensometer (FPBX) (Conroy et al., 1981; O'Rourke et al., 1977) consists of four major components (Fig. 11.8.4): a corrugated plastic tubing with metal rings, an induction probe, a cable reel and readout, and a survey tape and tripod. The corrugated plastic tubing in 20 ft (6.1 m) sections is flexible in the vertical direction, but rigid in the lateral direction, so that once attached to a borehole it is only sensitive to the vertical strata movement. Metal rings are firmly attached to the tubing at desired intervals. The gap between tubing and borehole wall is filled with pea gravel. The induction probe, 2 in. (50.8 mm) in diameter by 8 in. (203.2 mm) long, has a cable attached to a readout in a cable reel. If the cable is not graduated, a separate measuring tape is attached to the probe for distance measurement. During each measurement, the probe is lowered to the bottom of the borehole and raised gradually toward the surface. When the probe reaches the level of a metal ring, an inductive coupling between the ring and the probe is achieved and an electrical signal is transmitted to the cable reel, wherein it activates the buzzer. The exact location is then read from the measuring tape. The difference in reading between two successive measurements is the change in elevation or strata movement. An accuracy of 0.005 ft (1.5 mm) can be obtained.

Borehole extensometers (BOR-EX) consist of three main components: a displacement sensor, one or more anchors at various depths in the borehole, and a rod or wire each interconnecting a respective anchor with the displacement sensor. The displacement sensor is usually mounted inside a reference head (Fig. 11.8.5) located at the borehole collar and can be designed for electrical readout. The relative displacements of the rock, as transmitted to the rods, are measured by the displacement sensor as a change in the distance between an anchor within the borehole and the reference head at the borehole collar. A total of three extensometers can be connected together for monitoring overburden strata movement up to 500 ft (152.4 m) deep.

As relative displacement between the anchors and head assembly occurs, the location of the free ends of the rods in the head assembly move the same amount. By measuring the displacement between the free ends of the head assembly, the displacement of the anchors

relative to the head assembly is obtained. Displacement can be measured by the electrical head assembly and installing linear potentiometer displacement transducers.

Data acquisition and control system is a unit to collect, store, process, and output the data that is acquired from the anchors. The system scans all the anchors through rod or wire at a certain time defined by users and stores them into memory at the same frequency. The user can open and edit the data or transfer it into a computer (Fig. 11.8.6).

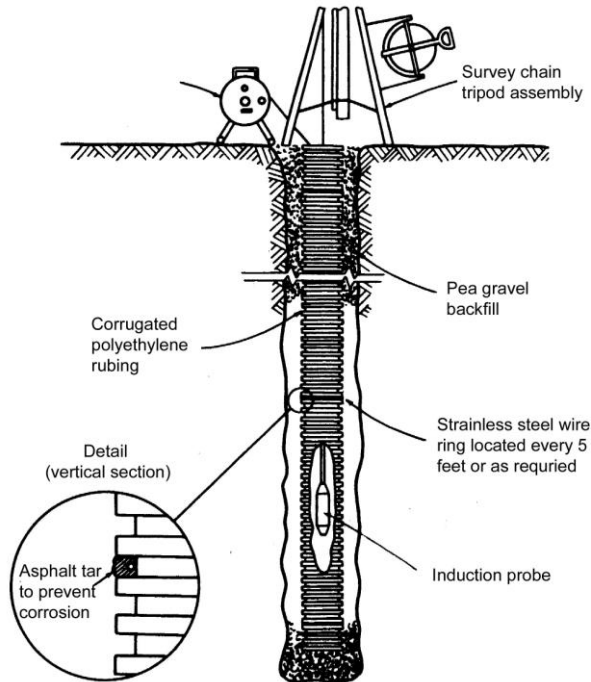


Fig. 11.8.4 Full profile borehole extensometer (FPBX) (Conroy et al., 1981)

#### 11.8.4 Full-Profile Borehole Inclinometer (FPBI)

The full profile borehole inclinometer (FPBI) (Conroy et al., 1981; O'Rourke et al., 1982; Khair et al., 1987a; Lin et al., 1987) measures the horizontal displacement profile by measuring the profile of the angle of inclination for a displaced flexible tubing (Fig. 11.8.7). It consists of three major components: a plastic pipe with two pairs of orthogonal internal grooves and a portable probe that rides on two pairs of guide wheels traveling on opposite grooves. The probe contains two accelerometers, mounted with their sensitive axes  $90^\circ$  apart so that their outputs can be used to determine the angle of inclination of the probe from the vertical line, and a battery-powered digital indicator connected by a distance-graduated electrical cable to the probe. During measurement, the probe is lowered to the bottom of the borehole and then raised by the cable in 2-ft (0.61 m) increments. At each increment, the angle of inclination is automatically displayed on the indicator. The process is repeated until the probe reaches the surface. The measurements must be performed in two orthogonal planes following the internal grooves of the tubing from which the true direction and magnitude of horizontal displacement can be determined. The standard inclinometer will operate through  $\pm 30^\circ$  from the vertical with a system accuracy of  $\pm 0.03$  in. (mm) per 100 ft (30.5 m).

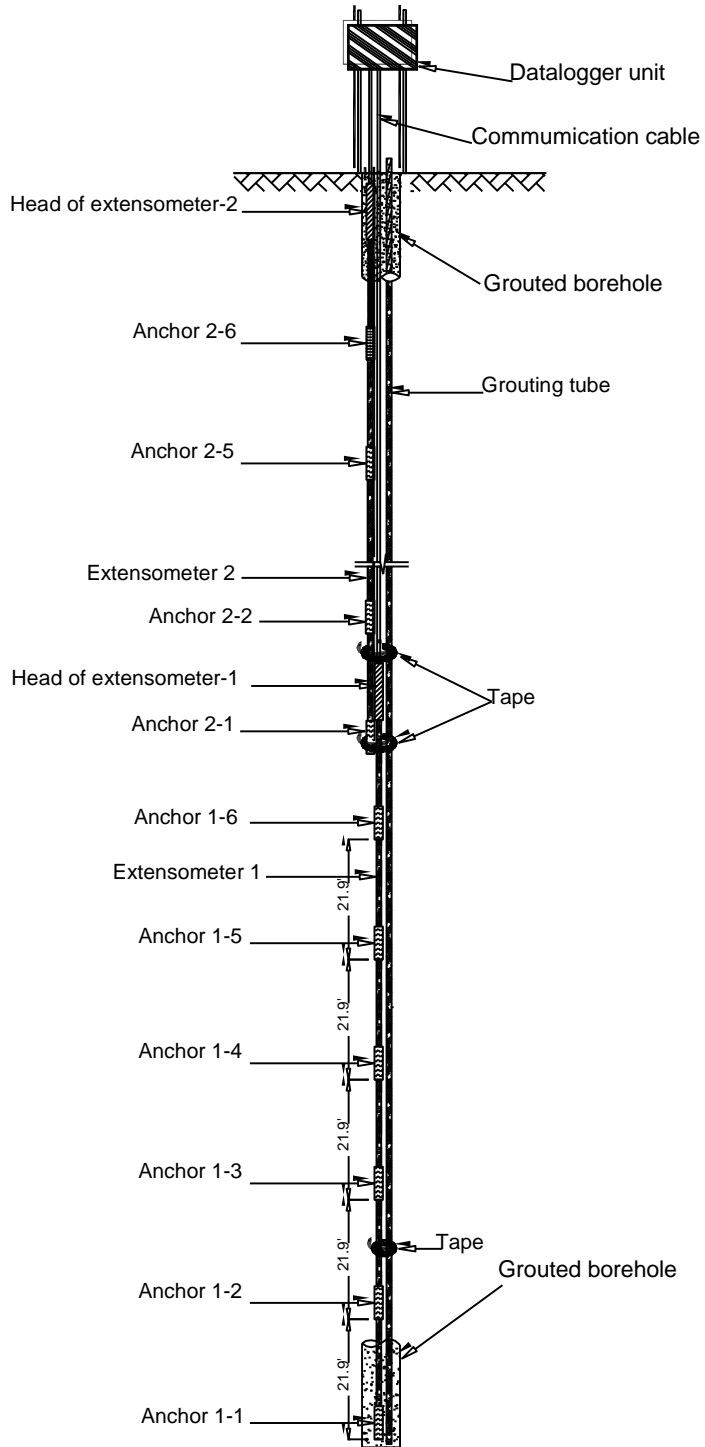


Figure 11.8.5 Instruments and installation of borehole extensometers BOR-EX



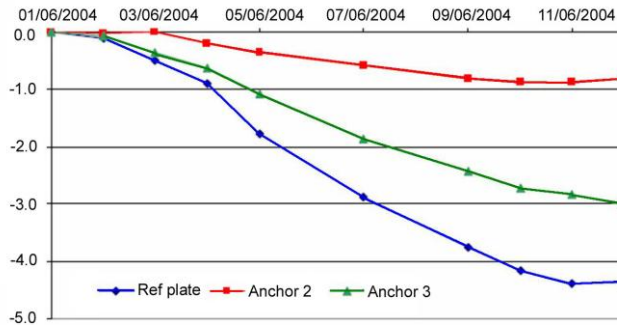


Fig. 11.8.6 Example of an extensometer (2 anchors) plot showing the capability of a BOR-EX

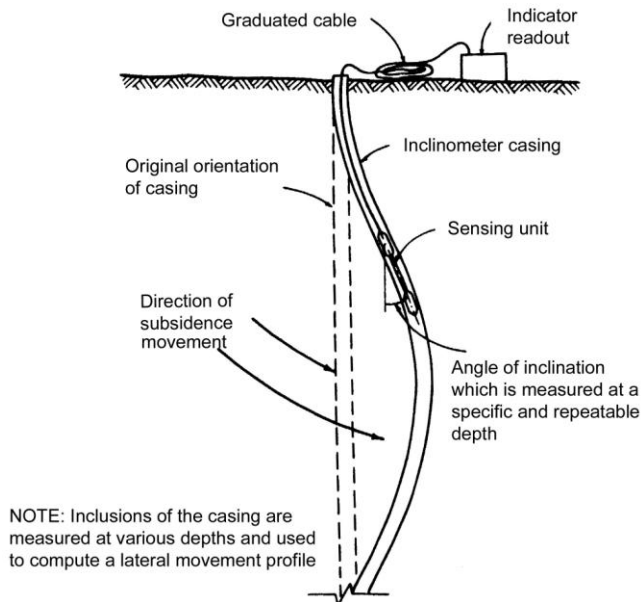


Fig. 11.8.7 Full profile borehole inclinometer (FPBI) (Conroy et al., 1981) and inclinometer (courtesy Slope Indicator, Inc.)

In order to augment the interpretative capacity at reduced cost, both the FPBX and the FPBI can be installed in a borehole (Fig. 11.8.8) (O'Rourke et al., 1982; Conroy and Gyarmaty, 1982 and 1983). The 3 in. (76.2 mm) diameter corrugated tube is installed in a 6 in. (162.4 mm) diameter borehole with the gap filled with pea gravel, and the metal rings are installed at 5 or 10 ft (1.5 or 3 m) intervals as desired. A 2 in. (50.8 mm) flexible tube is installed inside the corrugated tube for the inclinometer.

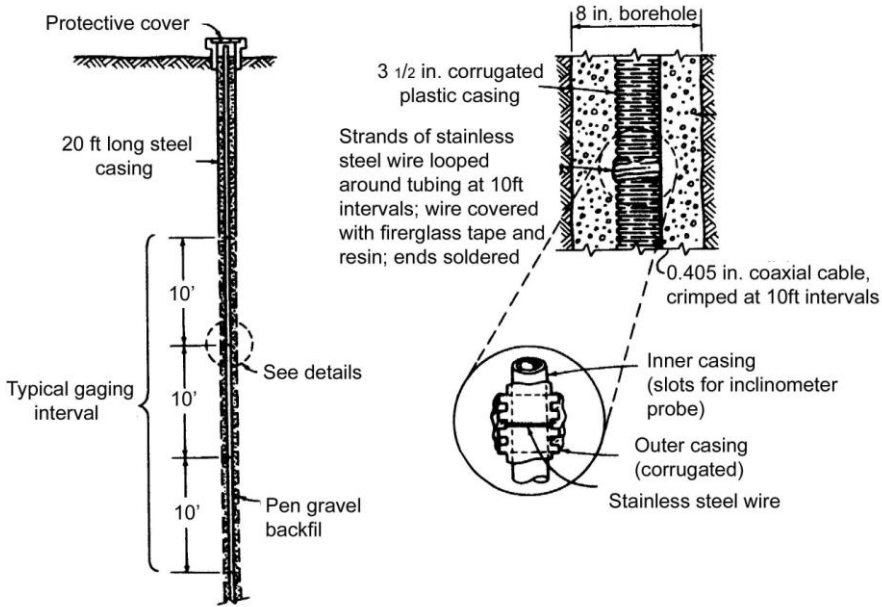


Fig. 11.8.8 Combined borehole installation of FPBX and FPBI (O'Rourke et al., 1982)

## 11.9 LONGWALL SHIELD MONITORING DEVICES

Two types of instrumentation are important for ground control in longwall shields: hydraulic leg pressure and DA ram position.

### 1. Hydraulic Pressure Transducers

The hydraulic pressure enters the open end of the transducer and causes deflection of the diaphragm (Fig. 11.9.1). The strain gauges mounted on the opposite side of the diaphragm will measure the amount of deformation and convert it to an electrical voltage change that can be monitored. The measured deformation can be calibrated to closely match the magnitude of pressure applied. With this sensor installed in each leg, the magnitude of leg pressure can be determined at any instant. This capability is used to implement the **positive set** of shield leg pressure. In this system after the introduction of high pressure fluid into the leg cylinder, its pressure continues to increase to a predetermined level, e.g., 110 bars, then the pilot signal is shut off automatically. But the high pressure fluid continues to build up until the setting load is reached. Therefore in an electrohydraulically controlled shield face, leg pressures are uniformly set all across the face, provided the cylinder and the hydraulic supply lines are not leaking.

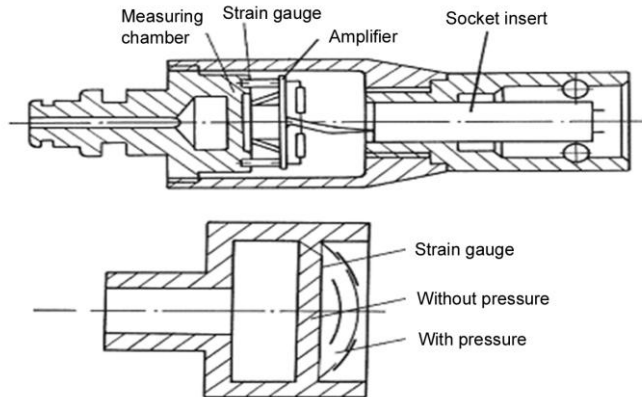


Fig. 11.9.1 Schematic of a hydraulic pressure transducer (Peng, 2006)

## 2. DA Ram Position Reed Rod Sensor

Figure 11.9.2 is a schematic drawing of a reed rod sensor for controlling the extension/retraction of DA ram mounted on a longwall shield. The reed rod contact switch is the most popular sensor for DA ram position measurement. The rod consists of a multitude of serial impedances of identical value. The reed contacts are soldered by one contact side to the connection points of the different impedances very much like the rungs of a ladder; the other side of the reed contact is electrically interconnected to form the sliding contact of a linear potentiometer.

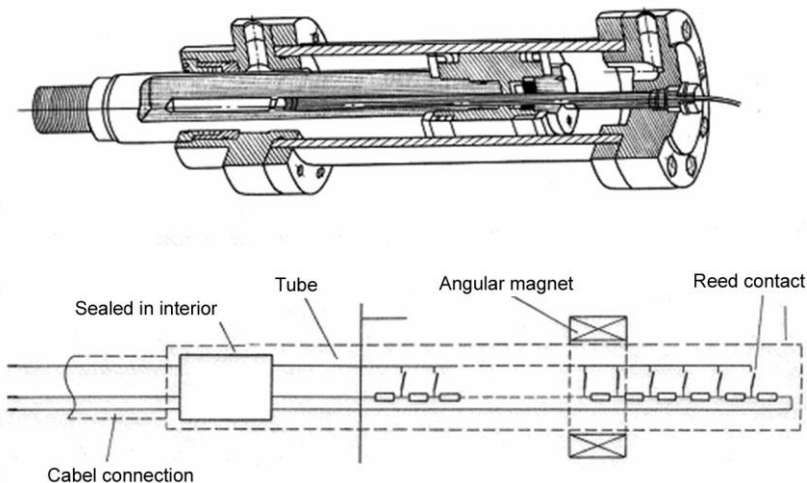


Fig. 11.9.2 Reed rod for measuring the stroke of DA ram: upper, cutaway view of DA ram and lower, principle of reed rod (Peng, 2006)

The impedance/reed combination is located within a steel tube and sealed against the internal hydraulic pressure. The measuring rod of the reed contacts are located inside and surrounded by an annular magnet that is built into the piston. As the piston moves, the reed contacts are switched on/off by the annular magnet as it follows the movement of the piston rod over the reed rod. This will change the resistance of the circuit. By monitoring the

resistance of the circuit, the exact location of the cylinder and, thus, the ram stroke can be determined. With this system it can be assured that the push-pull of DA ram is always to the full or predetermined length of stroke and ensures that shields and panline are always parallel in straight lines. With a reed rod sensor, the ram stroke is available in absolute value at any moment. The resolution and the measuring accuracy are better than 0.14 in. (3.6 mm). This, plus its precision, provides the basis for panline alignment, which in turn, provides the basis for automation for face alignment. Reed rod sensors are extremely reliable due to the absence of any moving electronic parts.

### 11.10 BOREHOLE PENETROMETOR

The borehole penetrometer was originally developed in Poland (Kidybinski, 1979) for measurement of in-situ rock strength. It was revised by Unrug (1994) first for application in NX (2-1/8 in. or 76 mm) holes and later for EX (1.5 in. or 38.1 mm) holes (Unrug, 1998; Unrug et al., 2001). It consists of a penetrometer head (a), hydraulic hoses (b), a pressure gauge (c), a pressure transducer (d), a hydraulic pump with pressure gauge (e), a double-acting cylinder (f), a moving plate for LVDT measurements (g), and a manual level bracket for pushing back the piston in the cylinder (Fig. 11.10.1). The indenter is the main part of the penetrometer and is used to load a rock at the borehole wall until its failure. The size of the indenter should be such that the wall rock fails in compression or shearing mode rather than by punching. Hence, a larger size is used for softer rock and coal, while a smaller one is used for harder rock such as sandstone and limestone. The penetrometer can be built for either strength testing or both strength and indenter penetration.

During testing, the indenter is pushed out to make contact with the wall rock of the borehole. The hydraulic pressure is gradually increased until the wall rock fails. At this moment the hydraulic pressure drops down instantaneously with an audible sound for brittle materials such as coal and harder rocks. The force or thrust in the indenter is recorded by the pressure transducer. The thrust in the indenter at which the wall rock fails is called the **penetration resistance**. It is recommended that 5 or 6 penetration tests should be performed at each testing horizon by turning the head around the circumference of the borehole and the results averaged to give the average penetration resistance. The penetration resistance is calibrated to UCS.

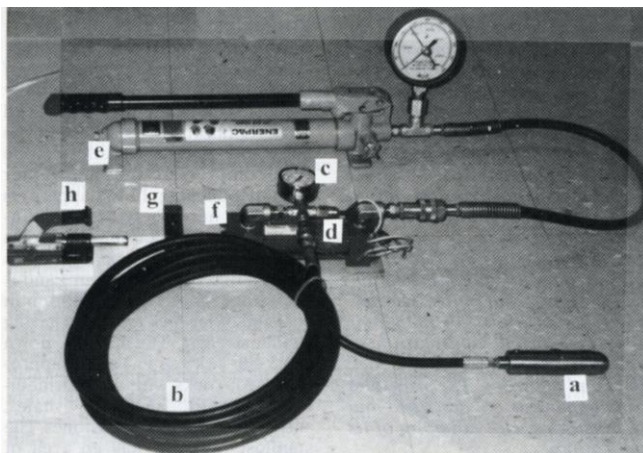


Fig. 11.10.1 Schematic of borehole penetrometer (Unrug et al., 2001)